Applied Geochemistry xxx (xxxx) 105359

Contents lists available at ScienceDirect

Applied Geochemistry

journal homepage: www.elsevier.com/locate/apgeochem

Major and trace element geochemistry of Permo-Triassic granitoids from NW Sonora, Mexico: Constraints on the origin of the Late Paleozoic-early Mesozoic Cordilleran magmatic arc along SW Laurentia

Alexander Iriondo [a, b, *], Harim E. Arvizu [a, 2], Francisco A. Paz-Moreno [c], Aldo Izaguirre [d], Andrés F. Velázquez-Santalíz [e, 1], Fernando Velasco-Tapia [e], Luis M. Martínez-Torres [f], Ofelia Pérez-Arvizu [a], Rufino Lozano-Santa Cruz [g]

[a] Centro de Geociencias, Universidad Nacional Autónoma de México, Campus Juriquilla, Querétaro, Qro, 76230, Mexico
[b] Department of Geosciences, University of Arizona, Tucson, AZ, 85721, USA
[c] Departamento de Geología, Universidad de Sonora, Blvd. Luis Encinas y Rosales s/n, Hermosillo, Sonora, 83000, Mexico
[d] Departamento de Ingeniería Civil y Ambiental, Instituto de Ingeniería y Tecnología, Universidad Autónoma de Ciudad Juárez, Av. del Charro 450, Cd. Juárez, Chihuahua, 32310, Mexico
[e] Facultad de Ciencias de la Tierra, Universidad Autónoma de Nuevo León, Carretera a Cerro Prieto km 8, Ex. Hacienda de Guadalupe, Linares N.L., 67700, Mexico
[f] Departamento de Geodinámica, Universidad del País Vasco, Apartado 644, E-48080, Bilbao, Spain
[g] Laboratorio Nacional de Geoquímica y Mineralogía, Instituto de Geología, Universidad Nacional Autónoma de México, Ciudad Universitaria, Alcaldía Coyoacán, Ciudad de México, 04510, Mexico

ARTICLE INFO

Editorial handling by Prof. M. Kersten

Keywords:
Calc-alkaline granitic suites
Permo-Triassic
Subduction magmatism
Cordilleran continental arc
NW Sonora
Mexico

ABSTRACT

Permo-Triassic granitoids (PTGs) (284–224 Ma) crop out in Sierra Los Tanques (SLT) and surrounding areas in NW Sonora, Mexico. Based on mineralogical and geochemical characteristics, the PTGs are subdivided into three main suites: melanocratic (MS), leucocratic (LS) and pegmatitic-aplitic (PAS) suites. MS has I-type signatures (mostly metaluminous: biotite and hornblende), while LS is weakly peraluminous with biotite, muscovite, and garnet. PAS is composed of garnet-bearing pegmatite-aplite dikes of Permo-Triassic age. MS is slightly older than LS based upon field relations and age dating. PAS cut both granitoid suites and local Paleoproterozoic banded gneisses. PTGs are petrologically and geochemically classified as granodiorites, granites, and quartz monzonites, with medium-to high-K calc-alkaline affinity, and volcanic-arc granite (VAG) signatures. The enrichment in LILE (such as K, Rb, Ba, Sr, and Pb) and LREE over HFSE and HREE, respectively, together with negative Nb, Ta, P, and Ti anomalies, suggest derivation from a crustal source in a continental arc setting. Trace-element ratios of Ba/Ta≫1000, Th/Yb > 1, and Th/Ta > 6–20 also support a setting in an active continental margin. All these geochemical features imply that crustal assimilation did play a major role in magma genesis. Crustal contamination is supported by field evidence, including xenoliths, stoped blocks, and roof pendants of Proterozoic basement rocks (Yavapai-type? crust). We propose that the PTGs from NW Sonora formed in a continental arc setting likely derived from the heat-fluxed melting of crustal material induced by mafic (basaltic?) underplating, thus the PTGs record the initiation of subduction and the generation of the early magmas in the nascent Late Paleozoic Cordilleran arc in SW Laurentia.

1. Introduction

Permo-Triassic granitoids (PTGs) are exposed in northwestern Mexico (284–224 Ma), and have been considered part of a nascent Cordilleran magmatic arc of Late Paleozoic age (Arvizu et al., 2009a; Arvizu and Iriondo, 2015) that extends from southwestern North America, across Mexico and Guatemala, and into northwestern South America (SW USA, e.g., Barth et al., 2000, 2001; Barth and Wooden, 2006; Cecil et al., 2019; Mexico and Guatemala, e.g., Torres et al., 1999; Solari et al., 2001, 2009, 2010; Dickinson and Lawton 2001; Weber et

* Corresponding author. Centro de Geociencias, Universidad Nacional Autónoma de México, Campus Juriquilla, Querétaro, Qro, 76230, Mexico.
E-mail address: iriondo@geociencias.unam.mx (A. Iriondo).
[2] Present address: Departamento de Ciencias de la Tierra, Universidad de Concepción, Víctor Lamas 1290, Casilla 160-C, Concepción, Chile.
[1] Former undergraduate student.

https://doi.org/10.1016/j.apgeochem.2022.105359
Received 2 February 2022; Received in revised form 26 May 2022; Accepted 30 May 2022
0883-2927/

al., 2005; Kirsch et al., 2012; Ortega-Obregón et al., 2014; Sarmiento-Villagrana et al., 2016; Coombs et al., 2020; NW South America–Colombia, Venezuela, and Ecuador, e.g., Viscarret et al., 2009; Cardona et al., 2010; Cochrane et al., 2014; Spikings et al., 2015; Van der Lelij et al., 2016; Rodríguez et al., 2017; Bustamante et al., 2017; Paul et al., 2018; Spikings and Paul, 2019; Piraquive et al., 2021a, b).

During Late Paleozoic time the southwestern margin of Laurentia underwent a tectonic transition from a northeast-southwest-trending passive margin, as evidenced by sedimentary records (e.g., Burchfiel and Davis, 1972), to an active subduction margin established along a reoriented northwest-southeast-trending continental margin (e.g., Stevens et al., 2005). Initiation of the Cordilleran magmatic arc in southwestern Laurentia is marked by intrusion of plutons along the west coast of North America during Permo-Triassic time (e.g., Barth et al., 1997; Barth and Wooden, 2006 and references therein; Arvizu et al., 2009a; Arvizu and Iriondo, 2015; Cecil et al., 2019). The northwest-southeast trending belt of Permo-Triassic plutons cuts across both the crystalline Proterozoic crust and the supracrustal depositional sequences of mostly Paleozoic age (Barth et al., 1990, 1997; Busby-Spera et al., 1990; Saleeby and Busby-Spera, 1992). The Cordilleran magmatic arc forms a southeast-trending belt extending from southern California and western Arizona (Miller et al., 1995; Barth et al., 1997; Cecil et al., 2019) through south-central Arizona and into northwestern and southern Sonora (e.g., Stewart et al., 1986; Riggs et al., 2003; Keppie et al., 2006; Arvizu et al., 2009a; Vega-Granillo et al., 2013; Arvizu and Iriondo, 2015; Sarmiento-Villagrana et al., 2016, 2018) and reappearing in NE Mexico (Coombs et al., 2020) and southern Mexico and Guatelama (e.g., Weber et al., 2005; Solari et al., 2009, 2010; Kirsch et al., 2012; Ortega-Obregón et al., 2014), to finally be found in NW South America (Colombia, Venezuela, and Ecuador; e.g., Spiking and Van der Lelij, 2022 and references therein).

Plutons in southwestern United States have ages between ca. 275–207 Ma, mostly Triassic in age, and show geochemical signatures related to subduction (e.g., Barth and Wooden, 2006 and references therein; Cecil et al., 2019). Plutons of the northern part of this belt intruded accreted oceanic terranes (Barth et al., 2011; Cecil et al., 2019), while further to the south in this belt Permo-Triassic plutons intruded the southwestern Laurentian craton and were emplaced into Proterozoic crust and its Paleozoic cratonal meta-sedimentary cover (e.g., Barth et al., 2000, 2001; Coleman et al., 2002; Arvizu et al., 2009b; Arvizu and Iriondo, 2015).

The PTGs (ca. 284–224 Ma) found in NW Sonora, Mexico (e.g., Arvizu et al., 2009a; Arvizu and Iriondo, 2015 and references therein) intruded Paleoproterozoic basement rocks (ca. 1.84–1.66 Ga) of SW Laurentia (Yavapai-type? crust) (Iriondo and Premo, 2011). Triassic plutonic rocks have also been documented in southern Sonora in the Sonobari Complex (ca. 249–203 Ma; Keppie et al., 2006; Sarmiento-Villagrana et al., 2016), which intrude Paleozoic metasedimentary rocks (Vega-Granillo et al., 2013; Sarmiento-Villagrana et al., 2016), extending this magmatic activity through the boundary between Sonora and Sinaloa states in NW Mexico. More recently, Coombs et al. (2020) proposed the presence of two age-distinct suites of plutonic rocks in NE Mexico; an older one between 294 and 274 Ma, supposedly related to arc magmatism associated with south-dipping subduction of oceanic crust underneath crust of Peri-Gondwana terranes (closing of the Rheic ocean), and a slightly younger pulse between 263 and 243 Ma, that they interpret as postcollisional magmatism (crustal anatexis) resulting after the diachronous collision of Laurentia and Gondwana to complete the final assembly of Pangea.

Extensive U–Pb zircon geochronology has provided the timing of the PTGs in NW Sonora (284–224 Ma; Arvizu and Iriondo, 2015) and elsewhere in the North America Cordillera. However, the petrogenesis of the PTGs in NW Sonora has not been elucidated in part due to limited rock exposures. In this paper, we present the first comprehensive geochemical study with the aim of shedding light on their origin and tectonic setting by presenting a set of major and trace element whole-rock geochemistry analyses of a well age-constrained group of PTGs. One of the main conclusions of this research is that the PTGs could have been generated by heat-fluxed melting of crustal material, induced by underplating of mafic (basaltic?) magmas derived from the lithospheric mantle wedge driven by subduction initiation of the Paleo-Pacific Plate beneath SW Laurentia margin during the Permo-Triassic time.

2. Previous geological studies in Permo-Triassic magmatism

2.1. Geochronology

Sierra Los Tanques (SLT) represents one of the largest outcrops of Permo-Triassic granitoids (PTGs) found in NW Mexico (Fig. 1a), and constitutes an interesting locality due to the occurrence of the youngest rocks of this magmatic activity with an age range extending throughout much of the Late Triassic (middle Norian, ca. 224 Ma), compared to the overall older arc plutons located further south in the Sierra San Francisco and Sierra Pinta with ages as old as 284 Ma and 275 Ma, respectively (Early to Middle Permian) (Table 1 and Fig. 2; Arvizu et al., 2009a; Velázquez-Santelíz, 2014; Arvizu and Iriondo, 2015; García-Flores, 2017). The main lithological unit in SLT corresponds to a set of granitoids of Permo-Triassic age (ca. 267–224 Ma; Fig. 2; Arvizu and Iriondo, 2015; García-Flores, 2017). The predominant lithologies include granodiorites and granites, followed by quartz monzonites (Table 1). PTGs are grouped into three lithologic suites according to their color index (Streckeisen, 1973, 1976; Le Maître et al., 2002): (1) melanocratic (MS), (2) leucocratic (LS), and (3) pegmatitic-aplitic (PAS) suites.

PTGs from Sierra Los Tanques, Sierra Pinta, and Sierra San Francisco in NW Sonora contain a large variety of rock assemblages with crystallization ages ranging from ca. 284 to 224 Ma (Artinskian–Norian) (Figs. 2 and 3a). The regional intrusive relations, supported by our field observations between the three granitoid suites, in-

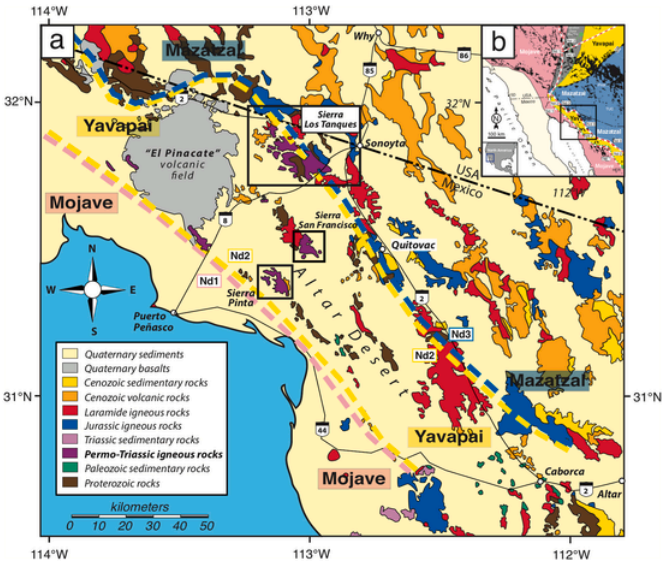

Fig. 1. (a) Lithologic map of northwestern Sonora and southwestern Arizona modified from Arvizu and Iriondo (2015) showing mountain ranges with Permo-Triassic granitoids discussed in the text (dark purple) and showing a tentative distribution of Paleoproterozoic basement provinces (Mojave, Yavapai and Mazatzal). (b) Inset: Paleoproterozoic basement provinces in SW Laurentia after Iriondo and Premo (2011) including rock outcrops (black) and the tentative Nd (red-dotted lines) and geochemical (green-dotted line) limits/boundaries among the provinces as defined in Iriondo et al. (2004). Abbreviations: MGSZ: Moore Gulch Shear Zone, LV: Las Vegas, LA: Los Angeles, SD: San Diego, PHX: Phoenix, TUC: Tucson, HER: Hermosillo. (For interpretation of the references to color in this figure legend, the reader is referred to the Web version of this article.)

Table 1
Sample location, classification, mineral assemblages, and U–Pb zircon ages for Permo-Triassic granitoids (PTGs) in Sierra Los Tanques (SLT) and adjacent areas in NW Sonora, Mexico.

Sample	Lat. (°N)[a]	Long. (°W)[a]	Rock type	Major minerals	Minor minerals	Accessory minerals	Suite	U–Pb age (Ma)
Sierra Los Tanques (Arvizu and Iriondo, 2015)								
TANW09-06	31°55′59″	113°09′33″	Biotite granodiorite	Pl + Kfs + Qtz + Bt	Ep	Ttn + Ap + Zrn + Opaq	Melanocratic	257 ± 5[b]
GneisSur-1	31°46′11″	113°03′10″	Gneiss	Qtz + Kfs + Pl + Bt	Ms + Ep + Chl	Ap + Zrn + Opaq	Leucocratic	255 ± 3[b]
CG09-10	31°56′44″	113°10′30″	Biotite monzogranite	Pl + Kfs + Qtz + Bt	Ep	Ttn + Ap + Zrn + Opaq	Melanocratic	254 ± 3[b]
TANSE09-01	31°46′14″	113°00′49″	Garnet-bearing leucocratic biotite-granodiorite (aplite)	Pl + Qtz + Kfs + Bt + Grt	N.A.	Ap + Zrn + Opaq	Leucocratic	254 ± 2[b]
TANSE-09	31°49′33″	112°58′21″	Leucocratic biotite-granodiorite	Pl + Qtz + Kfs + Bt	N.A.	Ttn + Ap + Zrn + Opaq	Leucocratic	252 ± 3[b]
GranCen-3	31°48′46″	113°07′51″	Two-mica leucocratic granodiorite	Pl + Qtz + Kfs + Bt + Ms	N.A.	Ap + Zrn + Opaq	Leucocratic	252 ± 2[b]
MICRO-3	31°56′35″	113°08′52″	Biotite quartz-monzodiorite	Pl + Kfs + Qtz + Bt	Ep	Ttn + Ap + Zrn + Opaq	Melanocratic	243 ± 2[b]
GranCen-5	31°52′52″	113°08′58″	Leucocratic biotite-granodiorite	Pl + Qtz + Kfs + Bt	N.A.	Ap + Zrn + Opaq	Melanocratic	240 ± 3[b]
TANW09-01	31°54′58″	113°09′30″	Two-mica leucocratic granodiorite	Pl + Qtz + Kfs + Bt + Ms	Ms	Ap + Zrn + Opaq	Leucocratic	238 ± 1[b]
TANC09-04	31°48′10″	113°06′41″	Leucocratic biotite-granodiorite	Pl + Qtz + Kfs + Bt	Ms + Ep	Ap + Zrn + Opaq	Leucocratic	231 ± 1[b]
LeucoCen-1	31°54′10″	113°08′47″	Biotite granodiorite	Pl + Qtz + Kfs + Bt + Grt	Ms + Chl	Ap + Zrn + Opaq	Leucocratic	226 ± 5[b]
GranCen-4	31°49′43″	113°06′25″	Two-mica leucocratic granodiorite	Pl + Qtz + Kfs + Bt + Ms	Ep	Ap + Zrn + Opaq	Leucocratic	224 ± 3[b]
Sierra Pinta (Arvizu et al., 2009a)								
PIN-07-1	31°27′46″	113°10′05″	Hornblende quartz-monzodiorite	Pl + Kfs + Qtz + Hbl	Bt + Ms + Ser + Ep + Chl	Ttn + Ap + Zrn + Opaq	Melanocratic	275 ± 4[c]
PIN-07-10	31°24′34″	113°07′28″	Two-mica granodiorite	Qtz + Kfs + Pl + Bt + Ms	Ser	Ttn + Ap + Zrn + Opaq	Melanocratic	271 ± 3[c]
PIN-07-12	31°24′26″	113°07′17″	Muscovite monzogranite	Qtz + Kfs + Ms + Pl	Chl + Ser	Ttn + Zrn + Opaq	Leucocratic	266 ± 3[c]
PIN-07-15	31°27′05″	113°10′46″	Two-mica monzogranite	Qtz + Kfs + Bt + Ms	Pl + Ep + Chl	Zrn + Opaq	Leucocratic	265 ± 3[c]
PIN-07-2	31°22′50″	113°08′24″	Muscovite monzogranite	Qtz + Kfs + Ms + Pl	Bt + Ser	Ttn + Zrn + Opaq	Leucocratic	259 ± 3[c]
PIN-07-4	31°23′31″	113°08′56″	Hornblende-biotite granodiorite	Pl + Qtz + Hbl + Bt	Ep + Ser	Zrn + Ttn + Ap + Opaq	Melanocratic	258 ± 3[c]
Sierra Los Tanques (García-Flores, 2017)								
TANSE09-17	31°47′19″	112°57′58″	Quartz-monzodiorite	Pl + Kfs + Qtz + Bt + Hbl	Chl	Ttn + Ap + Zrn + Opaq	Melanocratic	267 ± 2[d]
R-8 Km14	31°47′50″	112°58′46″	Quartz-monzodiorite	Pl + Kfs + Qtz	N.A.	Ttn + Ap + Zrn + Opaq	Melanocratic	266 ± 5[e]
CBNE09-28	31°49′32′	112°58′16″	Leucocratic Granodiorite	N.A.	N.A.	N.A.	Leucocratic	263 ± 10[d]
TANSE09-18	31°47′20″	112°57′56″	Monzogranite (pegmatite)	Pl + Qtz + Kfs + Bt + Grt	Ms	Ap + Zrn + Opaq	Pegmatite-Aplite	261 ± 2[d]
STAN09-04	31°47′27″	112°57′38″	Monzogranite (pegmatite)	Kfs + Pl + Qtz + Ms + Bt	N.A.	Ap + Zrn + Ttn + Opaq	Pegmatite-Aplite	261 ± 3[d]
STAN09-02	31°47′27″	112°57′32″	Granodiorite (pegmatite)	Pl + Qtz + Kfs + Bt + Ms	Ep + Chl + Ms	Ap + Zrn + Opaq	Pegmatite-Aplite	258 ± 2[d]
STAN09-03	31°47′27″	112°57′37″	Quartz-syenite (pegmatite)	Kfs + Pl + Qtz + Bt + Ms	N.A.	Ap + Zrn + Opaq	Pegmatite-Aplite	251 ± 3[d]
NEC09-50	31°54′49″	113°05′13″	Fine-grained leucocratic granite	N.A.	N.A.	N.A.	Leucocratic	251 ± 8[d]
CMIC09-23	31°48′31″	112°57′14″	Granodiorite	Pl + Qtz + Kfs + Bt	Ep + Chl + Ms	Ap + Zrn + Opaq	Melanocratic	250 ± 8[d]
1/99[d]13	N.A.	N.A.	Quartz-monzodiorite	Pl + Kfs + Qtz	N.A.	Ttn + Ap + Zrn + Opaq	Melanocratic?	N.A.
1/99[d]15A	N.A.	N.A.	Granodiorite	Pl + Qtz + Kfs	N.A.	Ap + Zrn + Opaq	Melanocratic?	N.A.
1/99[d]15B	N.A.	N.A.	Granodiorite	Pl + Qtz + Kfs	N.A.	Ap + Zrn + Opaq	Melanocratic?	N.A.
Sierra San Francisco (Velázquez-Santelíz, 2014)								
FRANS03	31°33′09″	113°03′42″	Granodiorite	Qtz + Pl + Kfs + Bt	Chl + Ser	Ttn + Zrn + Opaq	Melanocratic	284 ± 3[f]
SF09-05	31°40′29″	113°07′47″	Muscovite granodiorite (pegmatite)	Qtz + Pl + Kfs + Ms + Bt	Ser + Chl	Zrn + Opaq	Pegmatite-Aplite	264 ± 1[f]
FRANS01	31°30′47″	112°59′18″	Granodiorite	Pl + Qtz + Kfs + Bt	Chl + Ser	Ttn + Zrn + Opaq	Melanocratic	257 ± 17[f]
SF09-09	31°40′18″	113°08′15″	Granodiorite (pegmatite)	Qtz + Pl + Kfs + Ms + Bt	Chl	Zrn + Opaq	Pegmatite-Aplite	246 ± 1[f]
FRANS07	31°42′01″	113°11′05″	Biotite granodiorite	Pl + Qtz + Kfs + Bt + Hbl	Ep + Ms + Chl	Ttn + Ap + Zrn + Opaq	Melanocratic	244 ± 1[f]

Note: Abbreviations: Ap = Apatite, Bt = Biotite, Chl = Chlorite, Ep = Epidote, Grt = Garnet, Hbl = Hornblende, Kfs = K-feldspar, Ms = Muscovite, Opaq = Opaques, Pl = Plagioclase, Qtz = Quartz, Ser = Sericite, Ttn = Titanite, Zrn = Zircon.
N.A. = not available.

[a] Lat. = Latitude, Long. = Longitude. DATUM WGS84.
[b] 206 Pb/238U zircon ages by LA-ICPMS (Arvizu and Iriondo, 2015).
[c] 206 Pb/238U zircon ages by LA-MC-ICPMS (Arvizu et al., 2009a).
[d] 206 Pb/238U zircon ages by LA-ICPMS (García-Flores, 2017).
[e] 206 Pb/238U zircon age by SHRIMP-RG (García-Flores, 2017).
[f] 206 Pb/238U zircon ages by LA-ICPMS (Velázquez-Santelíz, 2014).

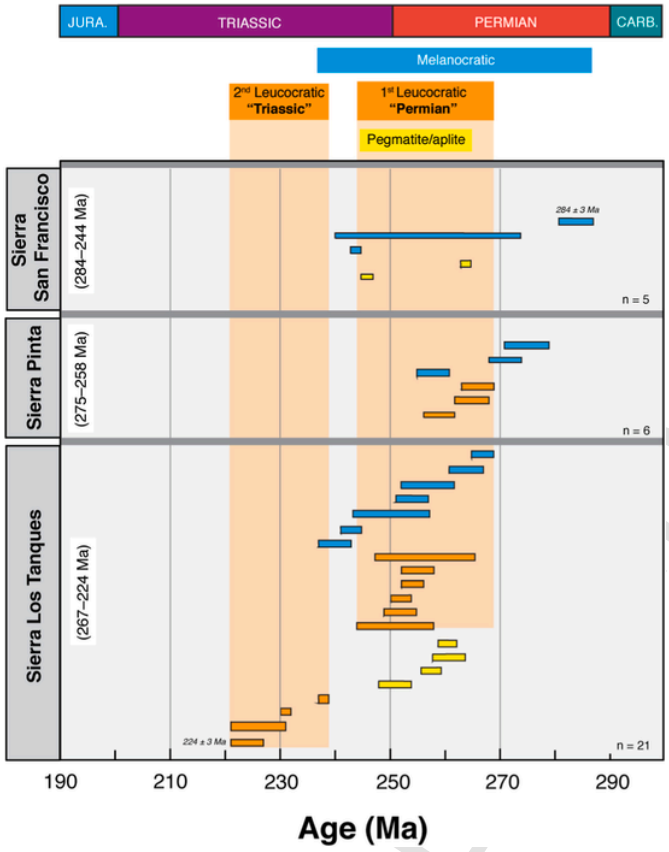

Fig. 2. Age diagram for U–Pb zircon geochronology of 32 Permo-Triassic granitoids (PTGs) from Sierra Los Tanques, Sierra Pinta, and Sierra San Francisco in NW Sonora, Mexico (age data from Table 1 and Arvizu and Iriondo, 2015). Melanocratic suite (MS) depicted in blue bars; Leucocratic suite (LS) in orange bars; Pegmatite-aplite suite (PAS) in yellow bars. Colored errors bars at 2 sigma. (For interpretation of the references to color in this figure legend, the reader is referred to the Web version of this article.)

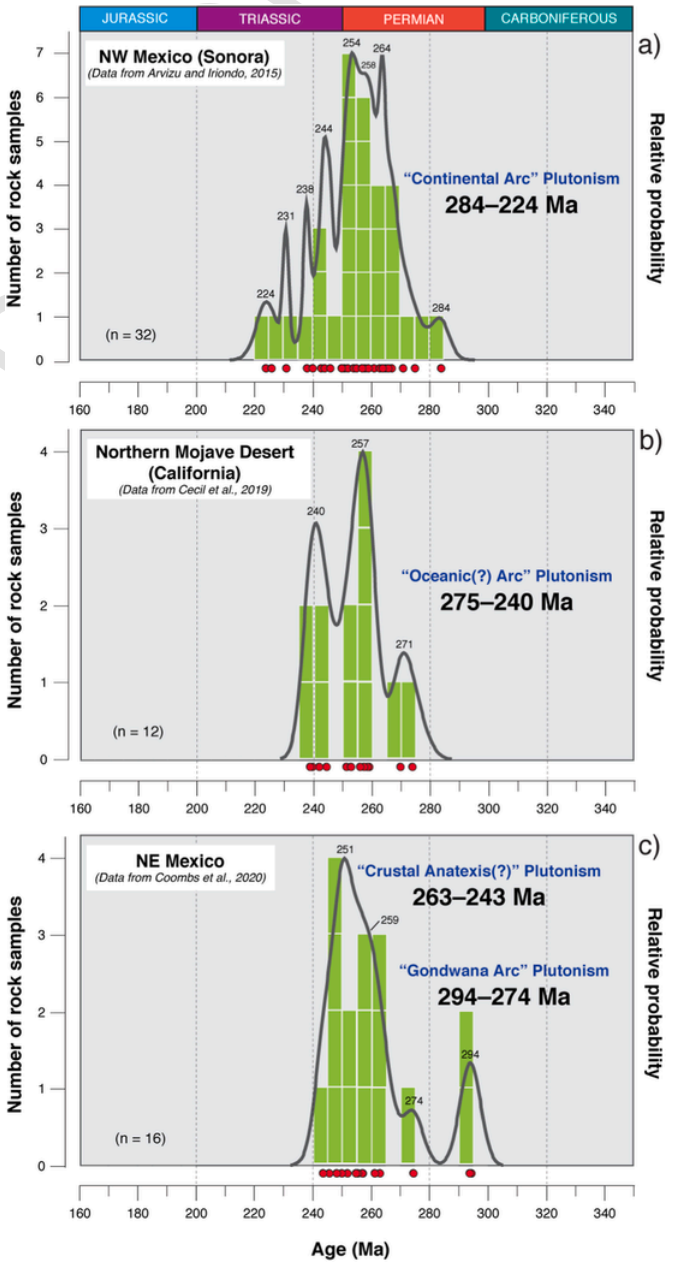

Fig. 3. Histogram and probability diagram of U–Pb zircon crystallization ages for (a) Permo-Triassic granitoids (PTGs) from NW Sonora (Table 1; data compiled from Arvizu et al., 2009a; Velázquez-Santelíz, 2014; Arvizu and Iriondo, 2015; García-Flores, 2017). (b) Permo-Triassic plutonic rocks from the northern Mojave Desert in California (Cecil et al., 2019) and (c) Permo-Triassic plutonic rocks from northeastern Mexico (Coombs et al., 2020).

dicate that the MS is older than the LS, and both suites being cut by the PAS (e.g., Fig. 4). This field evidence is supported by U–Pb zircon ages but, occasionally, the ages overlap within analytical error (Table 1; Arvizu and Iriondo, 2015; Velázquez-Santelíz, 2014; García-Flores, 2017). MS in the region is slightly older in all the study areas in NW Sonora (ca. 284–240 Ma; Table 1) and it is always intruded by the slightly younger LS granitoids (ca. 266–224 Ma). Rocks from both suites are cut by cm-to m-scale dikes of pegmatites and aplites of Permo-Triassic age (PAS; ca. 264–246 Ma; García-Flores, 2017), which occasionally contain abundant garnet (e.g., Fig. 5l). It is important to note that there is a group of 4 leucocratic granitoids in SLT that are significantly younger (238–224 Ma) than the other samples from the LS. PTGs intrude Paleoproterozoic quartz-feldspathic banded gneisses in SLT (ca. 1.7–1.6 Ga; Arvizu-Gutiérrez, 2012; García-Flores, 2017), and there are abundant enclaves derived from the Paleoproterozoic gneisses. Exposures of Precambrian rocks also occur as roof pendants or

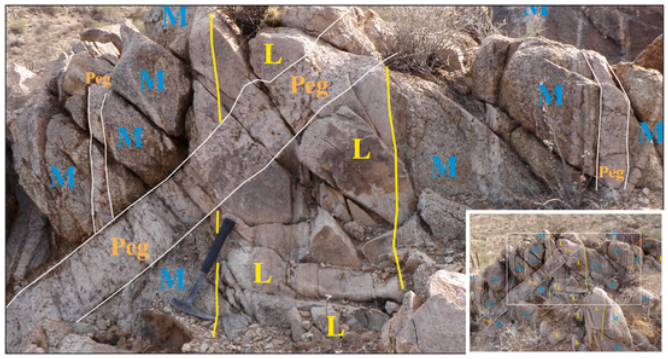

Fig. 4. Photograph showing a representative outcrop in Sierra Los Tanques with cross-cutting field relationships between the melanocratic (M) and leucocratic (L) suites as well as pegmatite dikes (Peg) cutting throughout. It is evident that the quartz monzodiorite (M: intrusive with darker color) is cut by a dike of leucocratic granodiorite (L: intrusive with lighter color). Both are slightly foliated but occasionally the leucocratic granodiorite appears to cut the fabric present in the quartz monzodiorite. Abundant pegmatite dikes (Peg) cross cut the melanocratic and leucocratic units; sometimes pegmatite dikes intrude along foliation of M and L. Nearby samples provide the following age constraint for the different suites: quartz monzodiorite (M) at 267 ± 2 Ma (TANSE09-17); leucocratic granodiorite (L) at 254 ± 2 Ma (TANSE09-01); quartz syenite pegmatite (Peg) at 251 ± 3 Ma (STAN09-03). (For interpretation of the references to color in this figure legend, the reader is referred to the Web version of this article.)

as large stoped blocks and xenoliths throughout the entire region (Arvizu-Gutiérrez, 2012; Arvizu and Iriondo, 2015).

2.2. Petrography

Detailed petrographic analysis of Permo-Triassic granitoids (PTGs) are presented in Arvizu-Gutiérrez (2012) and Arvizu and Iriondo (2015), but briefly, PTGs have phaneritic, locally porphyritic textures (Fig. 5a and b). MS is coarse-to medium-grained and hypidiomorphic-equigranular, containing the essential minerals plagioclase (45–55%), alkali feldspar (20–30%), quartz (10–25%), biotite (10–15%), and hornblende (<10%). Quartz grains are generally clustered between plagioclase with micrographic texture and occasional granophyric intergrowth. Plagioclase crystals show oscillatory zoning and sieve texture. Plagioclase also occurs as phenocrysts, which can reach 5 mm in length, showing polysynthetic twinning (Fig. 5a), and containing abundant inclusions of quartz and biotite. Mymerkitic texture occurs but is not common. Alkali feldspar sometimes occurs as late intergrowth with quartz (Fig. 5c). Occasionally, microcline is found and is partially resorbed (Fig. 5b). Ferromagnesian minerals include hornblende (often altered to chlorite and calcite) and biotite (altered to chlorite). Hornblende occurs as green crystals (Fig. 5d) and sometimes as dark brown crystals (varying from Ti-rich brown to Ti-poor green), ranging from 1 to 3 mm and sometimes more than 4 mm in size. Biotite is common in almost all samples and present brown and greenish yellowish pleochroic colors (Fig. 5e). Accessory minerals include zircon, apatite, titanite, and opaque minerals that are, most likely, iron oxides (Fig. 5k).

LS is coarse-to medium-grained and hypidiomorphic-equigranular, with grain sizes mostly in the range of 1–4 mm; slightly finer for the aplites and significantly larger for the pegmatites within the PAS. The leucocratic rocks of both the LS and PAS are dominated by quartz (30–55%), plagioclase (20–35%), K-feldspar (10–20%), biotite (<5%), muscovite (3–5%), and sometimes garnet (up to 1–3%). Plagioclase is mostly subhedral, and commonly shows polysynthetic twinning, locally as phenocryst, up to 8 mm in size. Myrmerkite texture was found in some samples. Sericite locally replaces plagioclase and/or K-feldspar (Fig. 5f). Biotite occurs as brownish to yellowish flakes and is partially replaced by chlorite in the groundmass (Fig. 5e and j). Muscovite occurs as a primary igneous mineral or as a replacement mineral (often replacing K-feldspar or plagioclase) (Fig. 5g and h). Garnet is mostly coarse-grained and subhedral in hexagonal to irregular sections (Fig. 5l). Zircon, apatite, and opaques (iron oxides?), and to a lesser extend titanite, occur as accessory minerals in these leucocratic rocks (suites LS and PAS). Secondary minerals are present, mainly chlorite replacing biotite, and epidote replacing orthoclase or plagioclase feldspars (Fig. 5i and j).

3. Geochemical analytical methods

Twenty-seven (27) samples of PTGs from Sierra Los Tanques (SLT) were collected from relatively fresh, unaltered outcrops to undertake whole-rock geochemical analyses. The samples were crushed in a steel jaw crusher to ≤0.5 cm-size pieces. The crushed rock was quartered by the manual cone and quartering method until an approximate volume of 50 ml was obtained, which was finally pulverized in an agate mill for the chemical analysis. Samples were processed at the Mineral Characterization Laboratory (CarMINLab) at Centro de Geociencias (CGEO, Universidad Nacional Autónoma de México–UNAM), Campus Juriquilla, Querétaro.

Whole-rock samples were analyzed for major- and trace-element compositions; the resulting geochemical data are given in Tables SD1−SD6 in the Supplementary Data Materials section. Major elements were analyzed on fused glass disks that were prepared by mixing thoroughly 0.8 g of sample powder with 7.2 g of $Li_2B_4O_7$–$LiBO_2$ flux in a 50:50 wt% mixture. Two drops of LiI (Lithium Iodide) solution in water (250 g/l) were added to the mixture as a non-wetting agent (NWA). The mixture was poured into a crucible made of 95% Platinum (PT)-5% Gold (AU), and heated to 1050 °C in an automated system Claisse M4 developed by Corporation Scientifique Claisse Inc., and equipped with three crucibles for simultaneous preparation of glass disks. The unknown samples were analyzed at the Laboratorio Nacional de Geoquímica y Mineralogía–Instituto de Geología, UNAM (LANGEM-IGL-UNAM) using a WD-XRF spectrometer ZSX Primus II developed by Rigaku Corporation. The calibration curves were constructed with 18 geochemical reference samples following the procedure described by Lozano and Bernal (2005). Trace element data were obtained using a Thermo Series XII Q-ICPMS at the Laboratorio de Estudios Isotópicos (LEI, CGEO, UNAM), following sample preparation and measurement procedures described by Mori et al. (2007). Trace elements concentrations in 4 samples were analyzed by INAA method (Instrumental Neutron Activation Analysis) at the U.S. Geological Survey laboratories in Denver, Colorado. Details of the INAA procedure may be found in Budahn and Wandless (2002).

4. Geochemistry results

Plutonic rock classification diagrams based on modal mineralogy (QAP; Streckeisen, 1976), and CIPW normative mineral parameters (ANOR vs. Q'; Streckeisen and Le Maître, 1979), show that the majority of PTGs fall in the fields for granodiorite, monzogranites and, to a lesser extent, quartz monzodiorite (Fig. 6). Rock classification based on major oxide geochemistry (De la Roche et al., 1980) also supports that the main lithologies of the PTGs are granodiorites and monzo- and syenogranites (Fig. 7a), and belong to the sub-alkaline series. Most of the PTGs comprise a low to medium-K suite (Peccerillo and Taylor, 1976, modified by Le Maître et al., 2002, Fig. 7b), and have compositions compatible with I-type granites with both metaluminous and peraluminous character (A/CNK <1.1; Chappell and White, 1974; Barbarin, 1999) (Fig. 7c). In the MALI diagram (Frost et al., 2001, Fig. 7d), the MS span the calcic to alkalic-calcic fields, with the majority being alkalic–calcic, while the LS and PAS plot mainly in the calc-alkalic field. On the Fe* index vs. SiO_2 plot (Fig. 7e) most of the MS plot in the ferroan series field, whereas the LS in most cases plot in the magnesian field. PTGs have a wide range of silica contents spanning from 60.52 to

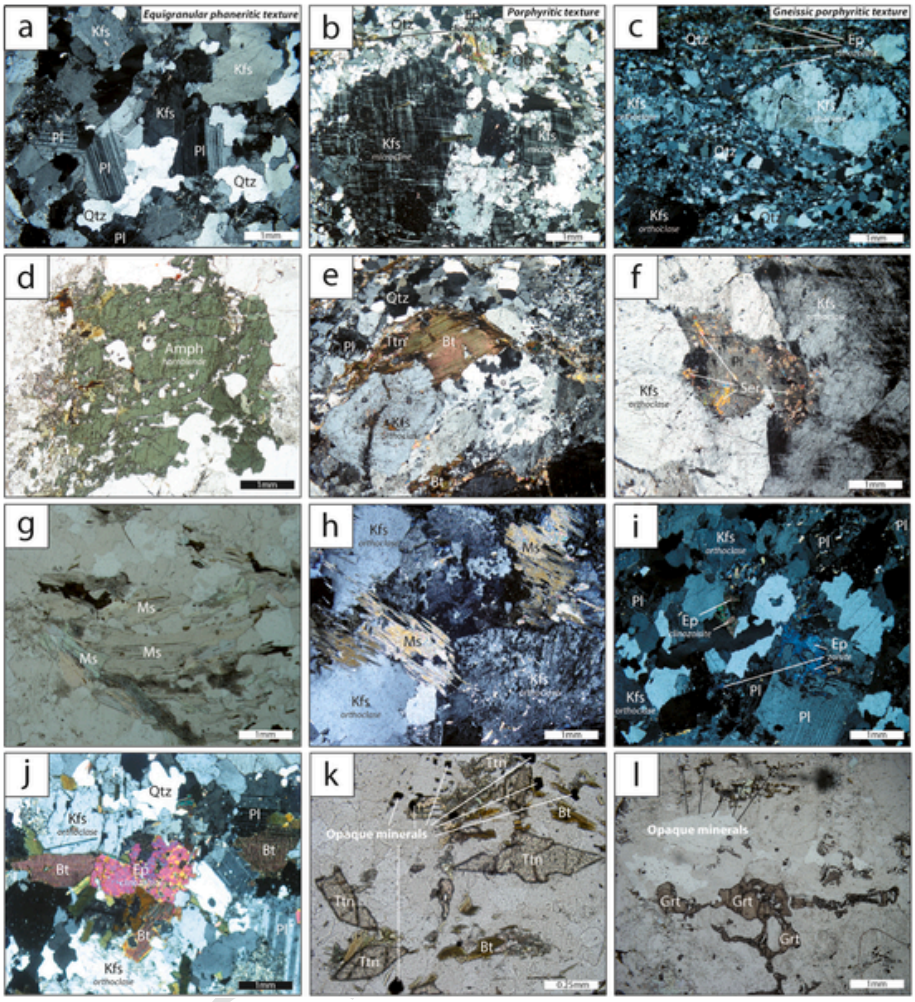

Fig. 5. Photomicrographs showing textures and mineralogy of representative samples of Permo-Triassic granitoids from Sierra Los Tanques (source Arvizu-Gutiérrez, 2012 and Arvizu and Iriondo, 2015). In (a), (b) and (c), representative textures seen in crossed polarized light (XPL). In (d) and (e), the dark minerals in the melanocratic suite of rocks include green hornblende and brown mica (biotite). (f) Sericite (or "white mica") is a common alteration mineral for both plagioclase and K-feldspar. In (g) and (h), muscovite crystals seen in plane polarized light (PPL) and XPL. This mineral commonly appears in the leucocratic suite as a primary mineral in (g) (PPL), although in some cases it is altered to chlorite. In (i) and (j), some secondary minerals, such as the epidote seen in XPL, are also present in granitoids, often chlorite replacing biotite, but saussurite (or epidote) is only formed through the alteration of Ca-plagioclase (i and j). (k) Rhombic crystals of titanite with high relief seen in PPL. (l) Garnet crystals showing high reliefs seen in PPL. Amph = Amphibole, Bt = Biotite, Ep = Epidote, Grt = Garnet, Kfs = K-Feldspar, Ms = Muscovite, Pl = Plagioclase, Qtz = Quartz, Ser = Sericite, Ttn = Titanite. (For interpretation of the references to color in this figure legend, the reader is referred to the Web version of this article.)

76.73 wt percent (Fig. 7b–e). Harker diagrams for TiO_2, Fe_2O_3, MnO and CaO show a negative correlation with SiO_2, whereas Al_2O_3, P_2O_5, and to a lesser extent MgO, abundances decrease with increasing SiO_2; correlations are not observed for the K_2O and Na_2O oxides (Fig. 8). This behavior is more accentuated in the MS.

Most trace elements plotted in Harker diagrams show negative or slightly negative correlations with respect to silica (Zr, Hf, U, Th, and Sr; Fig. 9), although some exhibit dispersion or remain constant without defining a clear tendency (e.g., Ba and Rb); Pb shows a slightly positive correlation. This scattered behavior is more accentuated in the LS and PAS samples.

According to the tectono-magmatic discrimination diagram for granitic rocks (Fig. 7f; Pearce et al., 1984), all the PTGs plot within the volcanic-arc granite (VAG) field. Relatively low Rb/Zr ratios and Nb concentrations further indicate a similarity to modern calc-alkaline continental arcs (Brown et al., 1984), plotting mainly in the field of normal maturity conditions of subduction-related rocks (Fig. 7g).

The high concentration of PTGs dots in the Nb/Zr vs. Sm/Yb diagram (He et al., 2010), coming mainly from Sierra Los Tanques, shows that the MS suite was generated by higher degrees of melting and at greater depth than the LS and PAS, where the PAS are the shallowest (Fig. 7h).

Primitive mantle-normalized incompatible multi-element spider diagrams for all the PTGs exhibit generally parallel patterns (Fig. 10), characterized by the enrichment of LILE such as Cs, Rb, Ba, K, Pb and Sr, with respect to HFSE, and LREE in relation to HREE. Chondrite-normalized REE distribution patterns for all the PTGs are plotted in Fig. 11. The MS exhibit moderately fractionated REE patterns ($[La/Yb]_N$ = 7.02–14.74; ΣREE = 25–220 ppm), flat heavy REE patterns, and have slight negative or positive Eu anomalies (Eu/Eu* = 0.77–1.64). The LS have strongly fractionated REE patterns ($[La/Yb]_N$ = 3.56–51.43; ΣREE = 13–231 ppm) with small to large positive Eu anomalies (Eu/Eu* = 0.80–2.63). The PAS is characterized by variably fractionated and unusual REE patterns ($[La/Yb]_N$ = 0.09–7.02), and have strong positive Eu anomalies (Eu/Eu* = 4.41–21.47).

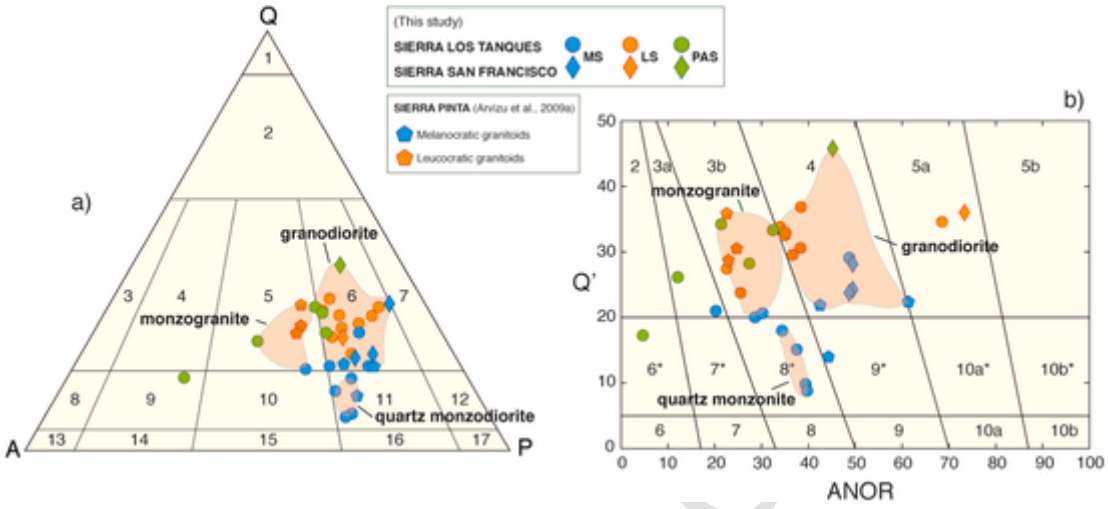

Fig. 6. Rock classification diagrams for Permo-Triassic granitoids (PTGs) from Sierra Los Tanques, Sierra Pinta, and Sierra San Francisco in NW Sonora (original point counting data from Arvizu-Gutiérrez, 2011). (a) modal mineralogy plotted in the QAP diagram of Streckeisen (1976). Q (quartz); A (feldspar); P (plagioclase). Fields as follow: 1—quartzolite; 2—quartz-rich granitoid; 3—alkali feldspar granite; 4—syenogranite; 5—monzogranite; 6—granodiorite; 7—tonalite; 8—quartz alkali feldspar syenite; 9—quartz syenite; 10—quartz monzonite; 11—quartz monzodiorite/quartz monzogabbro; 12—quartz diorite; quartz gabbro; quartz anorthosite; 13—alkali feldspar syenite; 14—syenite; 15—monzonite; 16—monzodiorite/monzogabbro; 17—diorite/gabbro/anorthosite. (b) CIPW normative mineral parameters: Q' = 100*Q/(Q + Qr + Ab + An) vs. ANOR = 100*An/(Or + An) diagram of Streckeisen and Le Maître (1979). Fields: 2—quartz alkali feldspar granite; 3a—syenogranite; 3b—monzogranite; 4—granodiorite; 5a—tonalite; 5b—tonalite; 6* = quartz alkali feldspar syenite; 7*—quartz syenite; 8*—quartz monzonite; 9*—quartz monzodiorite (An < 50); quartz monzogabbro (An > 50); 10a*—quartz diorite (An < 50); quartz gabbro (An > 50); anorthosite; 10b*—quartz diorite (An < 50); quartz gabbro (An > 50); anorthosite; 6—alkali felspar syenite; 7—syenite; 8—monzonite; 9—monzodiorite (An < 50); monzogabbro (An > 50); 10a—diorite (An < 50); gabbro (An > 50); 10b—diorite (An < 50); gabbro (An < 50). MS (melanocratic suite), LS (leucocratic suite), and PAS (pegmatitic-aplitic suite).

5. Discussion

5.1. Geochemical signature and tectonic setting: evidence for continental arc magmas and crustal assimilation/contamination

The enrichment in LILE and LREE relative to HFSE and HREE, particularly prominent negative anomalies for Nb, Ta, P and Ti of all the PTGs suites (Figs. 10 and 11), confirms the arc-related origin and strongly suggests that the PTGs are products of subduction-related magmas (Pearce, 1983; Brown et al., 1984; Wilson, 1989). These features lead to high Ba/Nb and Zr/Nb ratios, and low Ce/Pb ratios resembling the values of typical rocks from a magmatic arc setting (Stern, 2002). This setting is also supported by the Y vs. Nb tectonic diagram (Pearce et al., 1984, Fig. 7f), where all the PTGs plot in the volcanic-arc granite field (VAG). On the other hand, on the Rb/Zr vs. Nb diagram (Fig. 7g) all the PTGs represent 'the N-arc'– the normal continental arc granites generated in a normal stage of subduction (according to Brown et al., 1984). However, certain elemental ratios suggest the role of crustal assimilation/contamination. Most of the PTGs have La/Nb ratios > 0.5 varying between 1.2 and 4.7 for the MS, and higher values between 0.5 and 15.6 for the LS, with much lower values for the PAS (0.1–0.8). These values suggest that the PTGs magmas have been modified by various degrees of crustal assimilation during ascent or perhaps due to an extended residence time in the continental crust (e.g., Salter and Stracke, 2004). In addition, incompatible trace elements are also considered to determine crustal contamination. Most of the PTGs plot inside the active continental margin field in the Ta/Yb vs. Th/Yb diagram (Pearce, 1982, 1983, Fig. 12), indicating that their mantle source had subduction influence and the resulting magmas were affected by significant contamination with the lithosphere. Crustal assimilation/contamination affects Th more than Ta and Yb, so the samples which have crustal contamination show high Th/Yb values (Fig. 12; Moghazi, 2003; Gourgaud and Vincent, 2004). Only two samples from this study plot in the peraluminous field of the "S" type granites (Fig. 7c), with A/CNK > 1.1 (1.13 and 1.35), corresponding to the highest values in normative corundum > 1.0 (1.60 and 4.06, respectively, Tables SD3 and SD5), although they are devoid of modal garnet (Table 1). Modal garnet appears only in 3 of the 27 samples studied in the NW Sonora PTGs, with the lowest contents or without normative corundum and within the "I" type granites field. Modal titanite (accessory minerals) is present in most of the more differentiated MS and, also in the LS and PAS, although in smaller amounts, which are granitoids of two-mica and muscovite. In studies carried out by Richard (1991) on two-mica leucocratic granites in the Mazatán Metamorphic Core Complex from central Sonora, it was shown that rocks of this nature, with the presence of titanite, are only the differentiated phases of calc-alkalic series and not hyperaluminous rocks such as they were considered initially. Due to these characteristics, and those previously stated, we can consider that none of the studied PTGs from NW of Sonora meet the mineralogical and geochemical characteristics to be considered true peraluminous granitoids.

Lastly, in the MALI diagram of Frost et al. (2001) (Fig. 7d), the vast majority of the PTGs plot in the field of "Cordilleran granites", which represent a field drawn after plotting ~538 granitoid samples collected along the North America Cordillera, and presenting a wide range of ages, mostly Mesozoic, and with an ample range of silica contents. It is important to point out that a significant number of MS samples from NW Sonora plot above the field of "Cordilleran granites", in the field of alkalic-calcic compositions. However, a more recent geochemical data set presented by Barth and Wooden (2006) on Early-Middle Triassic granites (~250–230 Ma), collected in the southwestern Mojave Desert in California (pink field; Fig. 7d), requires to expand this field of granites to include more alkalic-calcic, and even alkalic compositions; therefore, the PTGs should be considered part of the "Cordilleran granites" field in the MALI vs SiO_2 space. Note that arc-related Permo-Triassic plutonism (274–243 Ma) in the northern Mojave Desert in California (green field; Fig. 7d; Cecil et al., 2019) presents calc-alkalic compositions similar to many of the PTGs from NW Sonora.

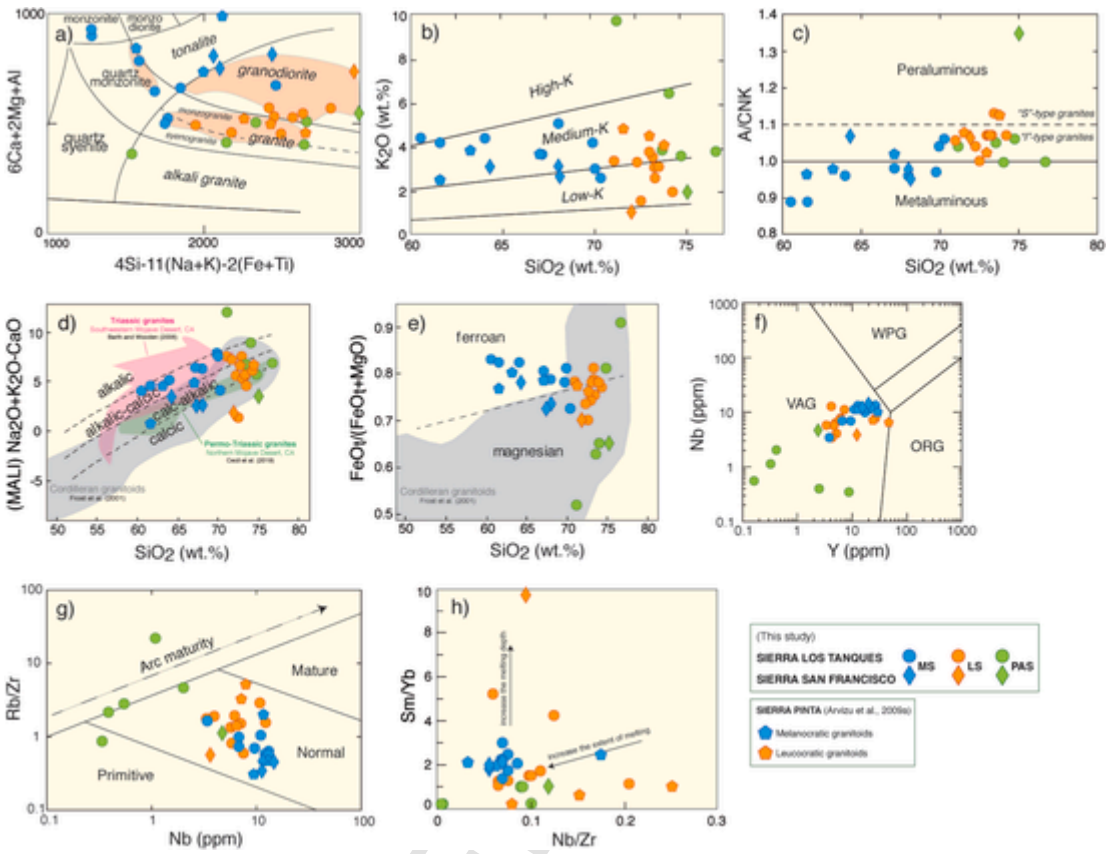

Fig. 7. Geochemical discrimination diagrams for Permo-Triassic granitoids (PTGs) from Sierra Los Tanques, Sierra Pinta, and Sierra San Francisco in NW Sonora. (a) Geochemical classification and nomenclature diagram for plutonic rocks according to De la Roche et al. (1980). (b) Diagram of K_2O vs. SiO_2 by Peccerillo and Taylor (1976) modified by Le Maître et al. (2002) showing the calc-alkaline magmatic series. (c) Plot of ASI versus silica (molecular ratio: $Al_2O_3/(CaO + Na_2O + K_2O)$ or ASI (Aluminum Saturation Index); A/CNK vs. SiO_2 separating S-type granites (ASI > 1.1) and I-type granites (ASI < 1.1). (d) Plot of modified alkali-lime index (MALI) ($[Na_2O + K_2O–CaO]$) against SiO_2, showing the various chemical magma types defined by Frost et al. (2001). (e) Binary diagram of SiO_2 vs. $FeO_t/(FeO_t + MgO)$ that discriminates between ferroan and magnesian magmatic series for granitoids according to Frost et al. (2001). (f) Tectonic discrimination plot Y vs. Nb according to Pearce et al. (1984). VAG: Volcanic Arc Granites; WPG: Within-Plate Granites; ORG: Ocean Ridge Granites (g) Rb/Zr vs. Nb diagram to determine the maturity of an arc (Brown et al., 1984). h). Nb/Zr vs. Sm/Yb diagram for the PTGs from NW Sonora. Vectors are after He et al. (2010). (For interpretation of the references to color in this figure legend, the reader is referred to the Web version of this article.)

5.2. The role of the Precambrian basement of NW Sonora: possible source for the PTGs

Source material of granitoids is one of the main subjects in igneous petrogenesis. Petrogenetic models for the origin of felsic arc magmas fall into two broad categories: (1) felsic arc magmas are derived from mafic (basaltic?) parent magmas by fractional crystallization or AFC processes (e.g., Grove and Donnelly-Nolan, 1986; Bacon and Druitt, 1988), and (2) mafic (basaltic?) magmas provide heat for the partial melting of crustal rocks (e.g., Roberts and Clemens, 1993; Tepper et al., 1993). Regarding the granitoids of this study, relative depletion of Ta and Nb (Brown et al., 1984), high concentration of LILE and LREE (Brown et al., 1984), and low concentration of Ti and P (Taylor and McLennan, 1985) are all typical criteria of rock generation from continental crustal materials (Chappell and White, 1992). Therefore, a derivation from crustal source is evident. Source of heat for crustal melting probably was from mantle-derived magma, which formed from partial melting of mantle wedge facilitated by dehydration of the subducted oceanic crust. Magmas generated in the mantle wedge must traverse the thick layer of sialic and incompatible element-enriched crust before reaching the surface. So, evident crustal assimilation can take place at this stage and contributing to the observed petrological and geochemical compositions of these granitoids.

Arvizu and Iriondo (2011, 2015) documented through cathodoluminescence images that Permo-Triassic zircons from PTGs from NW Sonora have textures that reveal abundant inherited cores. Large intra-sample εHf initial variations (−9.0 to −24.9) occurs in Permian granitoids from Sierra Pinta (Arvizu and Iriondo, 2011). Crustal melting may partially resorb and fractionate Hf from the older inherited zircon cores into the melt which crystallizes the zircon magmatic overgrowths (Cochrane et al., 2014). Newly crystallized zircon rims would thus record a locally mixed Hf isotopic signal, explaining the large spread in εHf(t) zircon compositions within plutonic samples.

Permian granitoids from Sierra Pinta studied by Arvizu and Iriondo (2011) show heterogenous zircon Hf-isotope compositions with negative εHf(t) values of −25 to −9 and Hf-crustal model ages (T_CDM) of 1.59–2.39 Ga suggesting the involvement of local Proterozoic basement rocks as magma sources. These Proterozoic rocks (ca. 1.7–1.6 Ga, 1.4 Ga, and 1.1 Ga; Iriondo et al., 2004, 2005; Nourse et al., 2005; Izaguirre et al., 2008; Arvizu et al., 2009b; Iriondo and Premo, 2011; Arvizu-Gutiérrez, 2012) crop out widely in SLT and surrounding regions in NW Sonora, Mexico (Fig. 1a and b). Most of the PTGs from NW Sonora contain abundant inherited zircons cores with ages varying in a range between ~1924 and 1071 Ma, with the principal age peaks at ca. 1.7–1.6 Ga, 1.4 Ga, and 1.1 Ga (Arvizu and Iriondo, 2015 and references therein), suggesting partial melting and/or assimilation of Paleoproterozoic basement. Therefore, we suggest that Proterozoic quartz-feldspathic gneisses and metasedimentary rocks are likely source materials of the precursor magmas that formed the Permo-Triassic granitoids (PTGs). We propose that the PTGs of NW Sonora formed in the

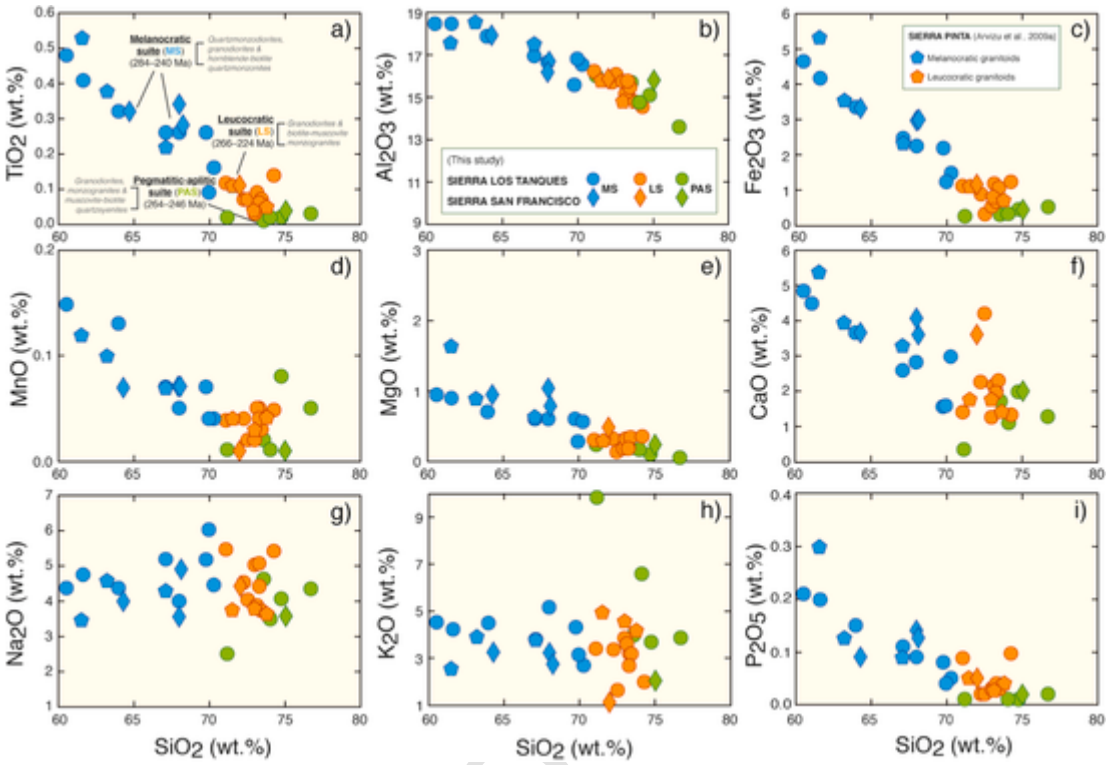

Fig. 8. Harker type variation diagrams for Permo-Triassic granitoids from NW Sonora showing abundances of major oxides (in weight percent). Age ranges and lithology types, for the different granitoid suites shown in (a), are from Arvizu and Iriondo (2015), and represent samples from Sierra Los Tanques, Sierra Pinta and Sierra San Francisco in NW Sonora.

early stage of an active continental margin dominated by crustal protoliths that underwent variable degrees of melting during increased heat-flux driven by basaltic underplating, contributing to the distinct geochemical compositions for the granitoids in NW Sonora.

5.3. Petrogenetic model for the PTGs of NW Sonora

Based on the geochemical data presented in this paper, together with previous geochronologic and isotopic studies (Arvizu et al., 2009a; Arvizu and Iriondo, 2011, 2015), we propose a tentative petrogenetic model for the emplacement of the PTGs of NW Sonora, Mexico (Fig. 13). In Late Paleozoic time, the southwestern Laurentian continental margin underwent a rearrangement of the margin's trend and a tectonic transition from passive, with a northeast-southwest trend, to an active subduction environment with a reoriented northwest-southeast-trending continental margin. Subduction initiation, and the associated continental magmatic arc, is indicated by the presence of Early Permian through Late Triassic plutons along a NW-SE–trending belt. These plutons were likely emplaced in a subduction-related compressional setting (Fig. 13), possibly as roots of the magmatic arc beneath the Proterozoic basement present in NW Sonora.

Proterozoic basement played a crucial role in the generation of the PTGs in NW Sonora. Previous studies in NW Mexico proposed that Paleoproterozoic rocks, with Yavapai-crust characteristics, had been able to act as a zone of crustal weakness (Paleoproterozoic sutures), so that the first magmas, generated by subduction during the Permo-Triassic period, rose, more easily, to the surface through these crustal discontinuities (Figs. 1 and 13) (Iriondo and Premo, 2011). This crustal weakness may have significantly conditioned the preferential location for the magmatism and the formation of the PTGs in NW Sonora (Fig. 1a; Sierra Blanca, Sierra San Francisco, Sierra Los Tanques, and Sierra Pinta). However, we interpret that in Permian time, the continental crust along the SW margin of Laurentia was thick, and primary magmas were likely ponded at the base of the crust. Compressional regimes commonly cause ponding of dense magmas at depth, whereas extension, or strike-slip motion, can provide conduits for the rapid ascent of magma into the arc, which means that more mafic, less differentiated magmas should reach surficial levels of the crust. Only during extensional episodes are the more primary magmas likely to reach the surface along faults or fault zones through a thinning crust in a continental arc. The crust/mantle interface was an effective density trap (underplating), and a great deal of magma should have assimilated crust at this level.

5.4. Timing of subduction initiation in different sectors of the Permo-Triassic magmatic arc in the SW North America Cordillera

It would be expected that earliest eastward-dipping subduction of the Paleo-Pacific oceanic plate would have started at different times along different sectors of the SW North America Cordillera before becoming a more mature and widespread subduction system. In addition, the resulting arc-related Permian granitoids would have formed after magmas crossed different basements types (oceanic vs continental crust) with different degrees of crustal assimilation/contamination. However, what appears common for all the plutonic rocks in the different sectors of the Cordilleran magmatic arc is their consistently similar arc-related geochemical signature (e.g., Barth and Wooden, 2006; Cecil et al., 2019; Coombs et al., 2020; this study).

There is still debate, but for the sector corresponding to the northern Mojave Desert in California, where the oldest granitoids occurred at ~275 Ma (Fig. 3b; Cecil et al., 2019), the basement that participated in the magma genesis appears to be of oceanic affinity (accreted oceanic terranes?) or just a transitional crust between oceanic to attenuated continental lithosphere (e.g., Miller et al., 1995; Barth et al., 2011; Cecil et al., 2019). Further to the south, in the southwestern Mojave Desert sector in California, Triassic magmas (~250–230 Ma) were emplaced into SW Laurentian Proterozoic crust and its Paleozoic supracrustal cover (e.g., Barth et al., 2000, 2001; Barth and Wooden,

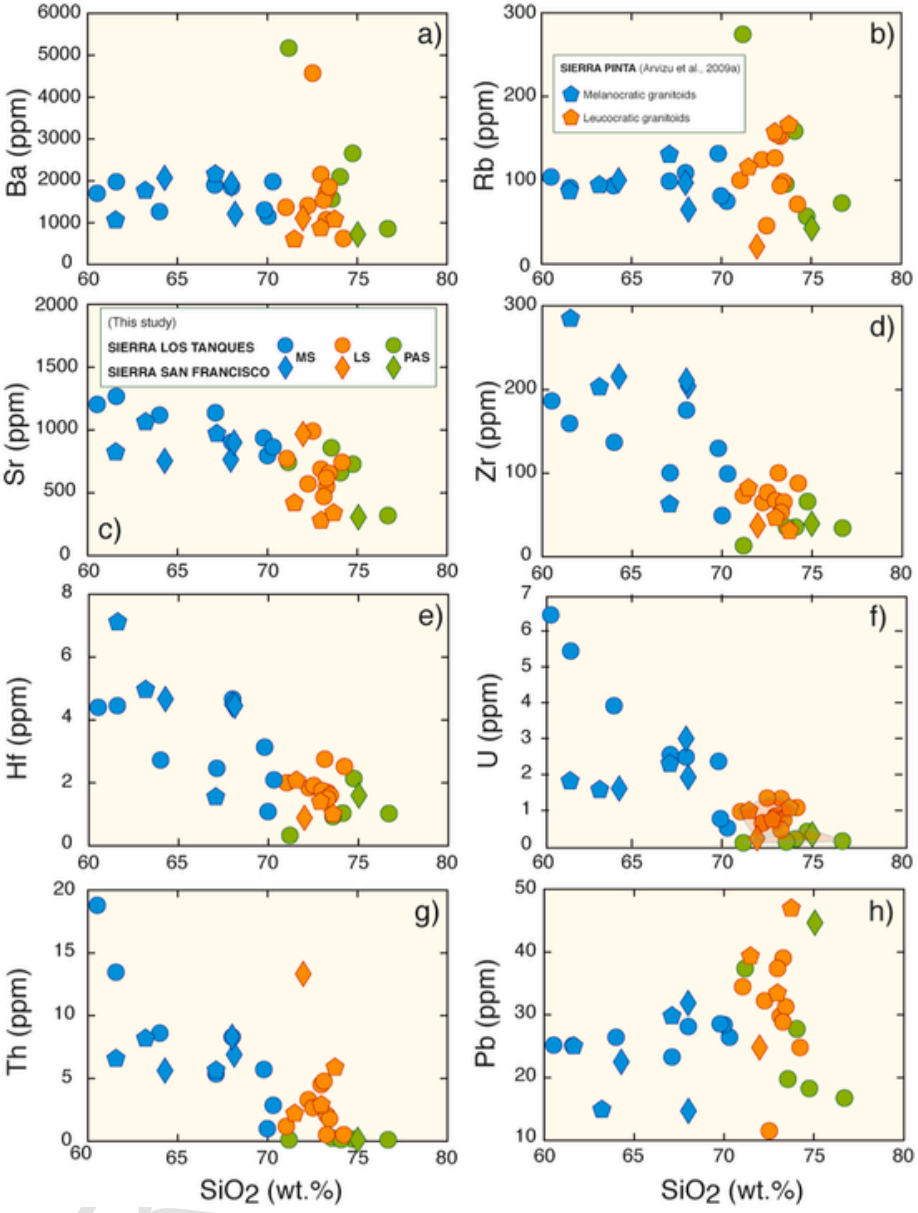

Fig. 9. Harker type variation diagrams for Permo-Triassic granitoids from NW Sonora showing abundances of trace elements (in ppm).

2006; Coleman et al., 2002), similarly to the Permo-Triassic granitoids present in NW Mexico (Sonora) sector where magmas assimilated abundant proportions of basement, more specifically from the Yavapai crust (Arvizu et al., 2009b; Arvizu and Iriondo, 2015). The oldest crystallization age obtained for Permian plutonic rocks in NW Sonora is 284 Ma (Table 1; Fig. 3a; Arvizu et al., 2009b; Arvizu and Iriondo, 2015), representing the oldest plutonic age recorded in the region and that could be connected to the onset of subduction for this sector of the Cordillera. In fact, detrital zircons with U–Pb ages between ~284 and 295 Ma (Artinskian-Sakmarian) are present in nearby Triassic siliciclastic sequences filling sedimentary basins in southwestern USA, like the Chinle Formation and Dockum Group sandstones (e.g., Riggs et al., 1996, 2003; Fox et al., 2005, 2006), and in sandstones from the Triassic El Antimonio and Barranca Groups in northern Mexico (e.g., González-León et al., 2009). These detrital igneous zircons suggest that subduction could have initiated even earlier in this part of the Cordillera, but the actual igneous rocks, that were sources of these detrital zircons, need to be found in the region.

In the NE Mexico sector of the Cordillera, plutonic magmatism associated with subduction should have started ~263 Ma (Fig. 3c; Coombs et al., 2020) and magmas assimilated crystalline basements of different peri-Gondwana terranes, similarly to what it is proposed for sectors further south in Mexico, and Guatemala, where Late Carboniferous-Permian arc magmas (~310–255 Ma) intruded Grenvillian-age Oaxaca and Paleozoic Acatlán basement complexes (e.g., Weber et al., 2005; Solari et al., 2009, 2010; Kirsch et al., 2012; Ortega-Obregón et al., 2014).

Lastly, crust formed during the Sunsas orogeny, in connection to the final assembly of Rodinia, of mostly Meso-to Neoproterozoic age, and Ordovician Famatinian crust, participated in the magma genesis of subduction-related Permian granitoids (~288–253 Ma) in the Colombian Cordillera sector. This is evidenced by the abundant presence of inherited zircons (zircon cores) in Permian plutonic rocks dated in the Guajira Peninsula, Sierra Nevada de Santa Marta, and in the central Cordillera Central (e.g., Cardona et al., 2010; Cochrane et al., 2014; Bustamante et al., 2017; Rodríguez et al., 2017; Piraquive et al., 2021a, b). Other sectors of the Cordilleran arc that extend to other parts of South America include Permo-Triassic arc-related magmas (~294–272 Ma) in Venezuela and Ecuador (e.g., Viscarret et al., 2009;

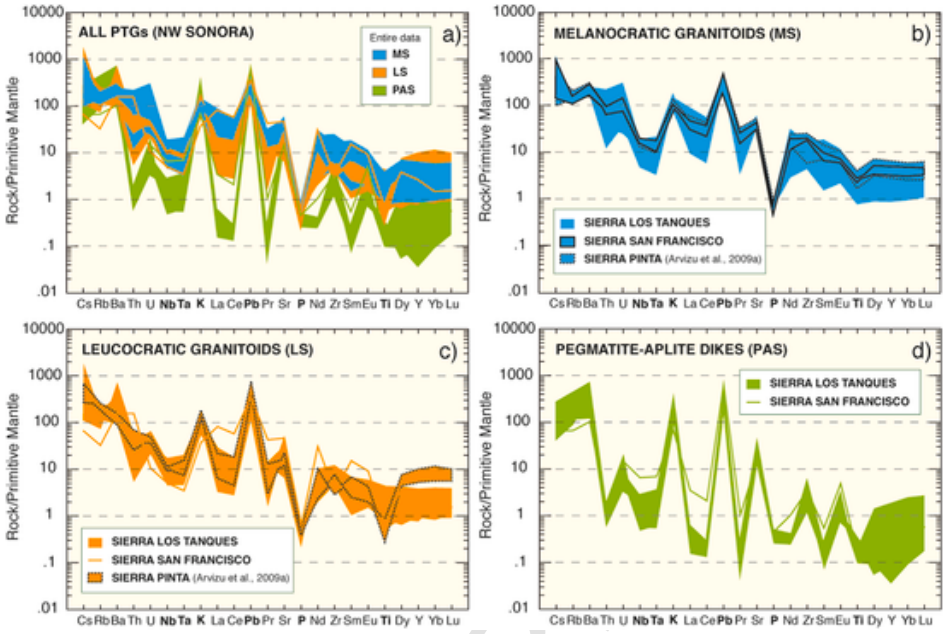

Fig. 10. Multi-element diagram normalized to primitive mantle (Sun and McDonough, 1989) showing both the melanocratic suite (MS) and leucocratic suite (LS), including the pegmatitic-aplitic suite (PAS) from Sierra Los Tanques and other localities in NW Sonora.

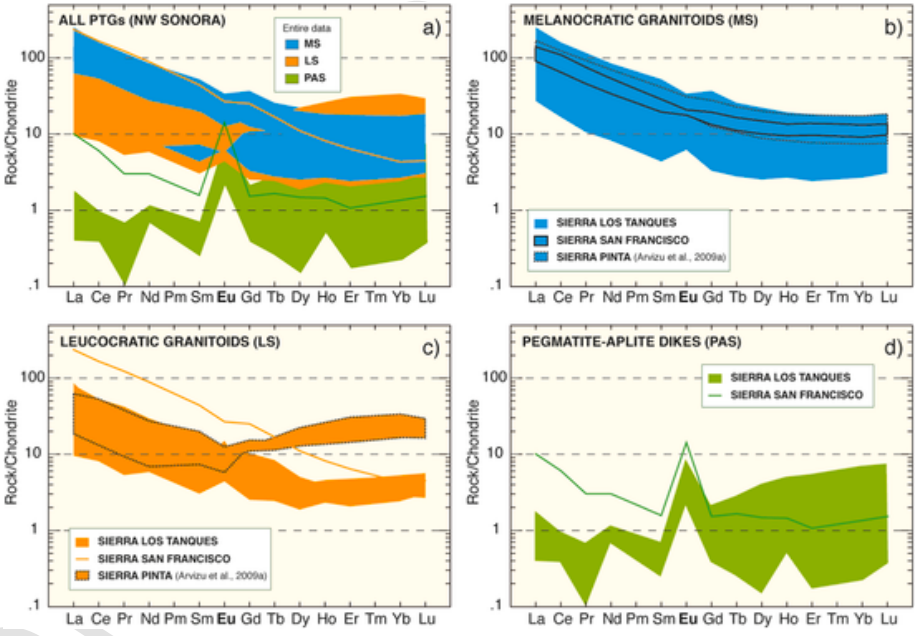

Fig. 11. Rare earth element diagrams (REE) normalized to chondrite (Sun and McDonough, 1989) for samples of PTGs from SLT and from other localities in NW Sonora. MS (melanocratic suite), LS (leucocratic suite), and PAS (pegmatitic-aplitic suite).

Spikings et al., 2015; Van der Lelij et al., 2016; Paul et al., 2018; Spikings and Paul, 2019).

6. Conclusions

Permo-Triassic granitoids (PTGs) (ca. 284–224 Ma) from NW Sonora are calc-alkaline rocks and classified as volcanic arc granites (VAG). The enrichment in crustal elements such as K, Rb, Ba, Sr, and Pb (LILEs) and LREE with respect to the HFSEs and HREE, with pronounced negative Nb, Ta, P, and Ti anomalies, suggest an arc-related origin and provide clear evidence for crustal assimilation.

These highly fractionated chemical features, together with the presence of inherited zircon cores, confirm that the PTGs were likely derived from the partial melting and/or assimilation of Paleo- and Mesoproterozoic basement. This assimilation of crustal material was verified from field evidence, with xenoliths, blocks, and roof pendants of Proterozoic gneissic, meta-granitic, and metasedimentary rocks (Yavapai-type? crust) present in the study area.

PTGs of NW Sonora represent the earliest arc-related magmatism in the nascent active continental margin formed during the east to northeastward-directed subduction initiation of the Paleo-Pacific Plate beneath the North America craton during Permo-Triassic time. We suggest that this tectonic event triggered the partial melting of the lithospheric mantle and subsequently mafic (basaltic?) underplating occurred at the base of the crust in a compressional setting, providing enough heat-flux to melt crustal material of Precambrian age. This

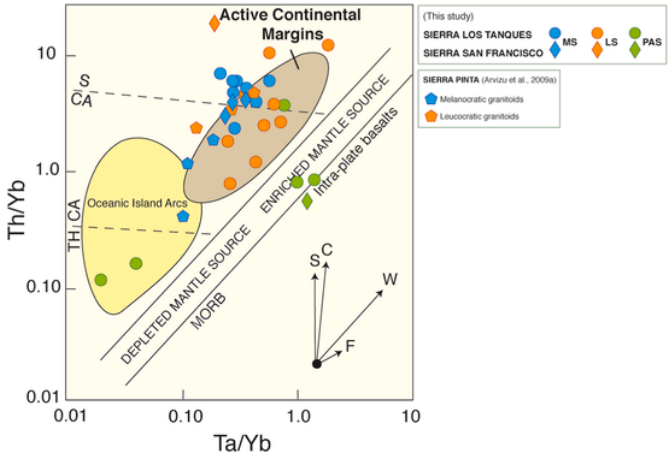

Fig. 12. Ta/Yb vs. Th/Yb plot showing the difference between magmas generated in different geodynamic environments. The vectors indicate the influence of the subduction components (S), intraplate enrichment (W), crustal contamination (C) and fractional crystallization (F). The dotted lines separate the boundaries of the tholeiitic (TH), calc-alkaline (CA), and shoshonitic (S) fields, according to Pearce (1983). The inclined continuous lines reflect the area occupied by magmas in equilibrium with the mantle. MS (melanocratic suite), LS (leucocratic suite), and PAS (pegmatitic-aplitic suite).

process contributed to the distinct geochemical compositions for the PTGs in NW Sonora, thus evolved isotopic and geochemical signatures were recorded in the early Cordilleran arc magmatism along the SW margin of Laurentia.

Uncited References

Boynton, 1983; Thornton and Tuttle, 1960.

Declaration of competing interest

The authors declare that they have no competing financial interests or personal relationships that could have appeared to influence the work reported in this paper.

Acknowledgements

This research was funded by the Consejo Nacional de Ciencia y Tecnología (CONACyT) grants CB129370 and CB82518, and PAPIIT-UNAM grant IN116709 provided to Iriondo. Arvizu acknowledges to CONACyT for providing a scholarship (grant no. 32533) during his Master's Thesis at Posgrado de Ciencias de la Tierra-UNAM. Lozano acknowledges CONACyT for the support provided for the development of the LANGEM infrastructure at UNAM. We are very thankful to Jon Nourse (Cal Poly Pomona) for providing a few plutonic samples from Sierra Los Tanques and to Jim Budahn (USGS-Denver) for analyzing them for trace elements using INAA. Jesus García Flores, a former undergraduate student at Universidad Estatal de Sonora-Hermosillo, is greatly acknowledged for providing well-dated granitoid samples from Sierra Los Tanques to be analyzed for major and trace element geochemistry. Thin sections for petrographic studies were prepared by Juan Tomás Vázquez Ramírez and Oscar Aguilar Moreno at the Centro de Geociencias-UNAM Juriquilla. Finally, we really appreciate comments and reviews from both Michael Kersten (Executive Editor) and Arturo Barron-Diaz (Guest Editor), and from two anonymous reviewers that helped us improve the manuscript significantly.

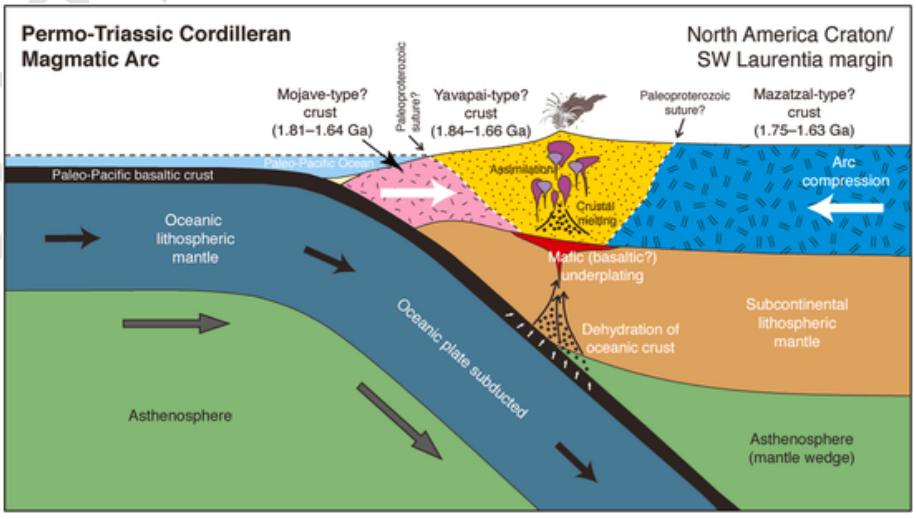

Fig. 13. Schematic cartoon showing tentative petrogenetic model for the formation of Permo-Triassic granitoids in NW Sonora, Mexico.

Appendix A. Supplementary data

Supplementary data to this article can be found online at https://doi.org/10.1016/j.apgeochem.2022.105359.

References

Arvizu-Gutiérrez, H.E., 2012. Magmatismo permo-triásico en el NW de Sonora, México: Inicio de la subducción y maduración de un margen continental activo [Tesis de Maestría]: Querétaro. Universidad Nacional Autónoma de México, p. 250.

Arvizu, H., Iriondo, A., 2011. Estudios isotópicos de Hf en zircones de granitoides pérmicos en el NW de México: posible evidencia de mezcla de magmas generados a partir de la fusión de múltiples fuentes corticales. Rev. Mex. Ciencias Geol. 28 (3), 493–518.

Arvizu, H., Iriondo, A., 2015. Control temporal y geología del magmatismo Permo-Triásico en Sierra Los Tanques, NW Sonora, México: evidencia del inicio del arco magmático cordillerano en el SW de Laurencia. Bol. Soc. Geol. Mex. 67 (3), 545–586.

Arvizu, H., Iriondo, A., Izaguirre, A., Chávez-Cabello, G., Kamenov, G.D., Solís-Pichardo, G., Foster, D.A., Lozano-Santa Cruz, R., 2009a. Rocas graníticas pérmicas en la Sierra Pinta en el NW de Sonora, México: magmatismo de subducción asociado al inicio del margen continental activo del SW de Norte América. Rev. Mex. Ciencias Geol. 26 (3), 709–728.

Arvizu, H., Iriondo, A., Izaguirre, A., Chávez-Cabello, G., Kamenov, G.D., Foster, D.A., Lozano-Santa Cruz, R., Solís-Pichardo, G., 2009b. Gneises bandeados paleoproterozoicos (~1.76–1.73 Ga) de la Zona Canteras-Puerto Peñasco: una nueva ocurrencia de rocas de basamento tipo Yavapai en el NW de Sonora, México. Bol. Soc. Geol. Mex. 61 (3), 375–402.

Bacon, C.R., Druitt, T.H., 1988. Compositional evolution of the zoned calcalkaline magma chamber of mount Mazama, crater Lake, Oregon. Contrib. Mineral. Petrol. 98, 224–256. https://doi.org/10.1007/BF00402114.

Barbarin, B., 1999. A review of the relationships between granitoid types, their origins and their geodynamic environments. Lithos 46, 605–626. https://doi.org/10.1016/S0024-4937(98)00085-1.

Barth, A.P., Wooden, J.L., 2006. Timing of magmatism following initial convergence at a passive margin, southwestern U.S. Cordillera, and ages of lower crustal magma sources. J. Geol. 114, 231–245. https://doi.org/10.1086/499573.

Barth, A.P., Tosdal, R.M., Wooden, J.L., 1990. A petrologic comparison of triassic plutonism in the san gabriel and mule mountains, southern California. J. Geophys. Res. 95, 20075–20096. https://doi.org/10.1029/JB095iB12p20075.

Barth, A.P., Tosdal, R.M., Wooden, J.L., Howard, K.A., 1997. Triassic plutonism in Southern California; southward younging of arc initiation along a truncated continental margin. Tectonics 6, 290–304. https://doi.org/10.1029/96TC03596.

Barth, A.P., Wooden, J.L., Coleman, D.S., 2001. SHRIMP-RG U-Pb zircon geochronology of Mesoproterozoic metamorphism and plutonism in the southwesternmost United States. J. Geol. 109, 319–327. https://doi.org/10.1086/319975.

Barth, A.P., Wooden, J.L., Coleman, D.S., Fanning, C.M., 2000. Geochronology of the Proterozoic basement of southwesternmost North America, and the origin and evolution of the Mojave crustal province. Tectonics 19, 616–629. https://doi.org/10.1029/1999TC001145.

Barth, A.P., Walker, J.D., Wooden, J.L., Riggs, N.R., Schweickert, R.A., 2011. Birth of the Sierra Nevada magmatic arc; Early Mesozoic plutonism and volcanism in the east-central Sierra Nevada of California. Geosphere 7, 877–897. https://doi.org/10.1130/GES00661.1.

Boynton, W.V., 1983. Cosmochemistry of the rare earth elements: meteorite studies. In: Henderson, P. (Ed.), Rare Earth Element Geochemistry. Elsevier, Amsterdam, pp. 63–114.

Brown, G.C., Thorpe, R.S., Webb, P.C., 1984. The geochemical characteristics of granitoids in contrasting arcs and comments on magma sources. J. Geol. Soc. 141 (3), 413–426. https://doi.org/10.1144/gsjgs.141.3.0413.

Budahn, J.R., Wandless, G.A., 2002. 02-223. Instrumental Neutron Activation by Abbreviated Count. U.S. Geological Survey Open File Report. Y1–Y9.

Burchfiel, B.C., Davis, G.A., 1972. Structural framework and evolution of the southern part of the Cordilleran orogen, western United States. Am. J. Sci. 272, 97–118. https://doi.org/10.2475/ajs.272.2.97.

Busby-Spera, C.J., Mattinson, J.M., Riggs, N.R., Schermer, E.R., 1990. The Triassic-Jurassic magmatic arc in the Mojave-Sonoran Deserts and the Sierran-Klamath region: similarities and differences in paleogeographic evolution. In: Harwood, D.S., Miller, M.M. (Eds.), Paleozoic and Early Mesozoic Paleogeographic Relations: Sierra Nevada, Klamath Mountains, and Related Terranes, vol. 225. Geological Society of America Special Paper, pp. 325–337. https://doi.org/10.1130/SPE255-p325.

Bustamante, C., Archanjo, C.J., Cardona, A., Bustamante, A., Valencia, V.A., 2017. U-Pb ages and Hf isotopes in zircons from parautochthonous mesozoic terranes in the western margin of Pangea: implications for the terrane configurations in the north Andes. J. Geol. 125, 487–500. https://doi.org/10.1086/693014.

Cardona, A., Valencia, V., Garzón, A., Montes, C., Ojeda, G., Ruiz, J., Weber, M., 2010. Permian to triassic I to S-type magmatic switch in the northeast Sierra Nevada de Santa Marta and adjacent regions, Colombian caribbean: tectonic setting and implications within Pangea paleogeography. J. S. Am. Earth Sci. 29, 772–783. https://doi.org/10.1016/j.jsames.2009.12.005.

Cecil, M.R., Ferrer, M.A., Riggs, N.R., Marsaglia, K., Kylander-Clark, A., Ducea, M.N., Stone, P., 2019. Early arc development recorded in Permian–Triassic plutons of the northern Mojave Desert region, California, USA. Geol. Soc. Am. Bull. 131 (5–6), 749–765. https://doi.org/10.1130/B31963.1.

Chappell, B.W., White, A.J.R., 1974. Two contrasting granite types. Pac. Geol. 8, 173–174.

Chappell, B.W., White, A.J.R., 1992. I-and S-type Granites in the Lachlan Fold Belt, vol. 272. Geological Society of America Special Paper, pp. 1–26. https://doi.org/10.1130/SPE272-p1.

Cochrane, R., Spikings, R., Gerdes, A., Ulianov, A., Mora, A., Villagómez, D., Putlitz, B., Chiaradia, M., 2014a. Permo-triassic anatexis, continental Rifting and the disassembly of western pangaea. Lithos 190–191, 383–402. https://doi.org/10.1016/j.lithos.2013.12.020.

Cochrane, R., Spikings, R., Gerdes, A., Winkler, W., Ulianov, A., Mora, A., Chiaradia, M., 2014b. Distinguishing between in-situ and accretionary growth of continents along active margins. Lithos 202–203, 382–394. https://doi.org/10.1016/j.lithos.2014.05.031.

Coleman, D.S., Barth, A.P., Wooden, J.L., 2002. Early to middle proterozoic construction of the Mojave province, southwestern United States. Gondwana Res. 5, 75–78. https://doi.org/10.1016/S1342-937X(05)70890-X.

Coombs, H.E., Kerr, A.C., Pindell, J., Buchs, D., Weber, B., Solari, L., 2020. Petrogenesis of the crystalline basement along the western Gulf of Mexico: postcollisional magmatism during the formation of Pangea. In: Martens, U., Molina-Garza, R.S. (Eds.), Southern and Central Mexico: Basement Framework, Tectonic Evolution, and Provenance of Mesozoic–Cenozoic Basins. Geological Society of America Special. Paper 546, 1–24. https://doi.org/10.1130/2020.2546(02).

De la Roche, H., Leterrier, J., Grandclaude, P., Marchal, M., 1980. A classification of volcanic and plutonic rocks using R1R2-diagram and major element analyses: its relation with current nomenclature. Chem. Geol. 29, 183–210. https://doi.org/10.1016/0009-2541(80)90020-0.

Dickinson, W.R., Lawton, T.F., 2001. Carboniferous to Cretaceous assembly and fragmentation of Mexico. Geol. Soc. Am. Bull. 113, 1142–1160. https://doi.org/10.1130/0016-7606(2001)113<1142:CTCAAF>2.0.CO;2.

Fox, J.D., Stair, K.N., Lehman, T.M., 2005. Detrital zircons in upper triassic strata of the upper Chinle and Dockum groups, New Mexico and Texas (abstract), in 101st Annual meeting of the cordilleran section. Geological Society of America: Geological Society of America, Abstract with Programs 38 (5), 10.

Fox, J.D., Anderson, C., Stair, K., Dickinson, W.R., 2006. Provenance contrasts revealed by U-Pb age populations of detrital zircons in Chinle sandstones of the four corners region, southwest US (abstract). In: 102nd Annual Meeting of the Cordilleran Section, Geological Society of America; 81st Annual Meeting of the Pacific Section, American Association of Petroleum Geologists, and the Western Regional Meeting of the Alaska Section: Geological Society of America, Abstracts with Programs, vol. 37, p. 46. 4.

Frost, B.R., Barnes, C., Collins, W., Arculus, R., Ellis, D., Frost, C.D., 2001. A geochemical classification for granitic rocks. J. Petrol. 42 (11), 2033–2048. https://doi.org/10.1093/petrology/42.11.2033.

García-Flores, J.R., 2017. Control temporal de eventos magmáticos presentes en Sierra Los Tanques en el NW de Sonora: Evidencia de asimilación de basamento en la generación de magmas [Tesis de Licenciatura]: Hermosillo. Universidad Estatal de Sonora, p. 140.

González-León, C.M., Valencia, V.A., Lawton, T.F., Amato, J., Gehrels, G.E., Leggett, W.J., Montijo-Contreras, O., Fernández, M.A., 2009. The lower Mesozoic record of detrital zircon U-Pb geochronology of Sonora, Mexico and its paleogeographic implications. Rev. Mex. Ciencias Geol. 26 (2), 301–314.

Gourgaud, A., Vincent, P.M., 2004. Petrology of two continental alkaline intraplate series at Emi Koussi volcano, Tibesti, Chad. J. Volcanol. Geoth. Res. 129, 261–290. https://doi.org/10.1016/S0377-0273(03)00277-4.

Grove, T.L., Donnelly-Nolan, J.M., 1986. The evolution of young silicic lavas at Medicine Lake Volcano, California: implications for the origin of compositional gaps in calc-alkaline series lavas. Contrib. Mineral. Petrol. 92, 281–302. https://doi.org/10.1007/BF00572157.

He, Q., Xiao, L., Balta, B., Gao, R., Chen, J., 2010. Variety and complexity of the Late-Permian Emeishan basalts: Reappraisal of plume–lithosphere interaction processes. Lithos 119, 91–107. https://doi.org/10.1016/j.lithos.2010.07.020.

Iriondo, A., Premo, W.R., 2011. Las rocas cristalinas proterozoicas de Sonora y su importancia para la reconstrucción del margen continental SW de Laurencia—la pieza mexicana del rompecabezas de Rodinia. In: Calmus, T. (Ed.), Panorama sobre la geología de Sonora, México 118 (2), 25–55. Universidad Nacional Autónoma de México, Instituto de Geología Boletín.

Iriondo, A., Premo, W.R., Martínez-Torres, L.M., Budahn, J.R., Atkinson, Jr, W.W., Siems, D.F., Guarás-González, B., 2004. Isotopic, geochemical, and temporal characterization of Proterozoic basement rocks in the Quitovac region, northwestern Sonora, Mexico: implications for the reconstruction of the southwestern margin of Laurentia. Geol. Soc. Am. Bull. 116, 154–170. https://doi.org/10.1130/B25138.1.

Iriondo, A., Martínez-Torres, L.M., Kunk, M.J., Atkinson, Jr, W.W., Premo, W.R., McIntosh, W.C., 2005. Northward Laramide thrusting in the Quitovac region, northwestern Sonora, Mexico: implications for the juxtaposition of Paleoproterozoic basement blocks and the Mojave-Sonora megashear hypothesis. In: Anderson, T.H., Nourse, J.A., McKee, J.W., Steiner, M.B. (Eds.), The Mojave-Sonora megashear hypothesis: Development, assessment, and alternatives 393, 631–669. Geological Society of America Special Paper. https://doi.org/10.1130/0-8137-2393-0.631.

Izaguirre, A., Iriondo, A., Wooden, J.L., Budahn, J.R., Schaaf, P., 2008. Paleoproterozoic orthogneisses from the cerro prieto area—a new addition to the Mexican Yavapai province in NW Sonora: Joint Annual meeting. Geological Society of America Abstracts with Programs 40 (6), 143–144.

Keppie, J.D., Dostal, J., Miller, B.V., Ortega-Rivera, A., Roldán-Quintana, J., Lee, J.W.K., 2006. Geochronology and geochemistry of the Francisco Gneiss: Triassic continental rift tholeiites on the Mexican margin of Pangea metamorphosed and exhumed in a Tertiary core complex. Int. Geol. Rev. 48, 1–16. https://doi.org/10.2747/0020-6814.48.1.1.

Kirsch, M., Keppie, J.D., Murphy, J.B., Solari, L., 2012. Permian–Carboniferous arc magmatism basin evolution along the western margin of Pangea: geochemical and

geochronological evidence from the eastern Acatlan Complex, southern Mexico. Geol. Soc. Am. Bull. 124, 1607–1628. https://doi.org/10.1130/B30649.1.
Le Maître, R.W., Bateman, P., Dudek, A., Keller, J., Lameyre, M., Le Bas, M.J., P, A., Schmid, R., Sørensen, H., Streckeisen, A., Woolley, A.R., Zanettin, B., 2002. A classification of igneous rocks and a glossary of terms. In: Recommendations of the International Union of Geological Sciences Subcommission on the Systematics of Igneous Rocks. Blackwell Scientific Publications, Oxford, p. 236.
Lozano, R., Bernal, J.P., 2005. Characterization of a new set of eight geochemical reference materials for XRF major and trace element analysis. Rev. Mex. Ciencias Geol. 22, 329–344.
Miller, J.S., Glazner, A.F., Walker, J.D., Martin, M.W., 1995. Geochronologic and isotopic evidence for Triassic-Jurassic emplacement of the eugeoclinal allochthon in the Mojave Desert region, California. Geol. Soc. Am. Bull. 107, 1441–1457. https://doi.org/10.1130/0016-7606(1995)107<1441:GAIEFT>2.3.CO;2.
Moghazi, A.M., 2003. Geochemistry of a Tertiary continental basalt suite, Red Sea coastal plain, Egypt: petrogenesis and characteristics of the mantle source region. Geol. Mag. 140 (1), 11–24. https://doi.org/10.1017/S0016756802006994.
Mori, L., Gómez-Tuena, A., Cai, Y., Goldstein, S.L., 2007. Effects of prolonged flat subduction on the Miocene magmatic record of the central Trans-Mexican Volcanic Belt. Chem. Geol. 244, 452–473. https://doi.org/10.1016/j.chemgeo.2007.07.002.
Nourse, J.A., Premo, W.R., Iriondo, A., Stahl, E.R., 2005. Contrasting Proterozoic basement complexes near the truncated margin of Laurentia, northwestern Sonora-Arizona international border region. In: Anderson, T.H., Nourse, J.A., McKee, J.W., Steiner, M.B. (Eds.), The Mojave-Sonora megashear hypothesis: Development, assessment, and alternatives 393, 123–182. Geological Society of America Special Paper. https://doi.org/10.1130/0-8137-2393-0.123.
Ortega-Obregón, C., Solari, L., Gómez-Tuena, A., Elías-Herrera, M., Ortega-Gutiérrez, F., Macías-Romo, C., 2014. Permian–Carboniferous arc magmatism in southern Mexico: U-Pb dating, trace element and Hf isotopic evidence on zircons of earliest subduction beneath the western margin of Gondwana. Int. J. Earth Sci. 103, 1287–1300. https://doi.org/10.1007/s00531-013-0933-1.
Paul, A.N., Spikings, R.A., Ulianov, A., Ovtcharova, M., 2018. High temperature (>350°C) thermal histories of the Long lived (>500 Ma) active margin of Ecuador and Colombia: apatite, titanite and Rutile U-Pb thermochronology. Geochem. Cosmochim. Acta 228, 275–300. https://doi.org/10.1016/j.gca.2018.02.033.
Pearce, J.A., 1982. Trace element characteristics of lavas from destructive plate boundaries. In: Thorpe, R.S. (Ed.), Andesites: Orogenic Andesites and Related Rocks. John Wiley & Sons, Chichester, U.K., pp. 525–548.
Pearce, J.A., 1983. Role of the sub-continental lithosphere in magma genesis at active continental margins. In: Hawkesworth, C.J., Norry, M.J. (Eds.), Continental Basalts and Mantle Xenoliths. Shiva Press, Nantwich, U.K., pp. 230–249.
Pearce, J.A., Harris, N.B.W., Tindle, A.G., 1984. Trace element discrimination diagrams for the tectonic interpretation of granitic rocks. J. Petrol. 25 (4), 956–983. https://doi.org/10.1093/petrology/25.4.956.
Peccerillo, A., Taylor, S.R., 1976. Geochemistry of Eocene calc-alkaline volcanic rocks from the Kastamonu area, northern Turkey. Contrib. Mineral. Petrol. 58, 63–81. https://doi.org/10.1007/BF00384745.
Piraquive, A., Kammer, A., Bernet, M., Cramer, T., von Quadt, A., Gómez, C., 2021a. Neoproterozoic to Jurassic tectono-metamorphic events in the Sierra Nevada de Santa Marta massif, Colombia: insights from zircon U-Pb geochronology and trace element geochemistry. Int. Geol. Rev. 1–33. https://doi.org/10.1080/00206814.2021.1961317.
Piraquive, A., Kammer, A., Gómez, C., Bernet, M., Muñoz-Rocha, J.A., Quintero, C.A., Laurent, O., von Quadt, A., Peña-Urueña, M.L., 2021b. Middle-late triassic metamorphism of the Guajira Arch-basement: insights from zircon U–Pb and Lu–Hf systematics. J. S. Am. Earth Sci. 110, 103397. https://doi.org/10.1016/j.jsames.2021.103397.
Richard, D., 1991. De la subduction à l'extension, intra-continentale; plutonisme et gisements de tungstène de l´Etat de Sonora (Mexique), Centre d'Orsay, Université de Paris-Sud, Ph. D. dissertation, p. 775 (unpublished).
Riggs, N.R., Lehman, T.M., Gehrels, G.E., Dickinson, W.R., 1996. Detrital zircon link between headwaters and terminus of the Upper Triassic Chinle-Dockum paleoriver system. Science 273, 97–100.
Riggs, N.R., Ash, S.R., Barth, A.P., Gehrels, G.E., Wooden, J.L., 2003. Isotopic age of the black forest bed, petrified forest member, Chinle Formation, Arizona: an example of dating a continental sandstone. Geol. Soc. Am. Bull. 115 (11), 1315–1323. https://doi.org/10.1130/B25254.1.
Roberts, M.P., Clemens, J.D., 1993. Origin of high-potassium, calcalkaline, I-type granitoids. Geology 21 (9), 825–828. https://doi.org/10.1130/0091-7613(1993)021<0825:OOHPTA>2.3.CO;2.
Rodríguez, G., Zapata, G., Arango, M.I., Bermúdez, J.G., 2017. Caracterización petrográfica, geoquímica y geocronología de rocas granitoides pérmicas al occidente de La Plata y Pacarní–Huila, Valle Superior del Magdalena–Colombia. Bol. Geol. 39 (1), 41–68. https://doi.org/10.18273/revbol.v39n1-2017002.
Saleeby, J.B., Busby-Spera, C.J., 1992. Early Mesozoic tectonic evolution of the western U.S. Cordillera. In: Burchfiel, B.C., Lipman, P.W., Zoback, M.L. (Eds.), The Cordilleran Orogen: Conterminous U.S. (Geology of North America, G- 3. Geological Society of America, Boulder, Colorado, pp. 107–168.
Salter, V.J.M., Stracke, A., 2004. Composition of the depleted mantle. G-cubed 5, Q05B07. https://doi.org/10.1029/2003GC000597.
Sarmiento-Villagrana, A., Vega-Granillo, R., Talavera-Mendoza, O., Vidal-Solano, J.R., 2016. New age constraints on magmatism and metamorphism of the Western Sonobari Complex and their implications for an earliest Late Cretaceous orogeny on northwestern Mexico. Rev. Mex. Ciencias Geol. 33 (2), 170–182. https://doi.org/10.22201/cgeo.20072902e.2016.2.494.
Sarmiento-Villagrana, A., Vega-Granillo, R., Talavera-Mendoza, O., Salgado-Souto, S.A., Gómez-Landa, J.R., 2018. Geochemical and isotopic study of Mesozoic magmatism in the Sonobari Complex, western Mexico: implications for the tectonic evolution of southwestern North America. Geosphere 14 (1), 304–324. https://doi.org/10.1130/GES01540.1.
Solari, L.A., Dostal, J., Ortega-Gutiérrez, F., Keppie, J.D., 2001. The 275 Ma arc-related La Carbonera stock in the northern Oaxacan Complex of southern Mexico: U-Pb geochronology and geochemistry. Rev. Mex. Ciencias Geol. 18 (2), 149–161.
Solari, L.A., Ortega-Gutiérrez, F., Elías-Herrera, M., Schaaf, P., Norman, M., de León, R.T., Ortega-Obregón, C., Chiquín, M., Ical, S.M., 2009. U-Pb zircon geochronology of palaeozoic units in western and Central Guatemala: insights into the tectonic evolution of Middle America. Geological Society, London, Special Publication 328 (1), 295–313. https://doi.org/10.1144/SP328.12.
Solari, L.A., Ortega-Gutiérrez, F., Elías-Herrera, M., Gómez-Tuena, A., Schaaf, P., 2010. Refining the age of magmatism in the Altos cuchumatanes, western Guatemala, by LA–ICPMS, and tectonic implications. Int. Geol. Rev. 52, 977–998. https://doi.org/10.1080/00206810903216962.
Spikings, R.A., Paul, A., 2019. The Permian—Triassic History of Magmatic Rocks of the Northern Andes (Colombia and Ecuador): Super-continent Assembly and Disassembly, vol. 15p. Servicio Geológico Colombiano: Bogotá, Colombia.
Spikings, R., Van der Lelij, R., 2022. The geochemical and isotopic record of Wilson cycles in northwestern South America: from the Iapetus to the caribbean. Geosciences 12 (1), 5. https://doi.org/10.3390/geosciences12010005.
Spikings, R., Cochrane, R., Villagomez, D., Van der Lelij, R., Vallejo, C., Winkler, W., Beate, B., 2015. The geological history of northwestern South America: from pangaea to the early collision of the caribbean large igneous province (290–75 Ma). Gondwana Res. 27 (1), 95–139. https://doi.org/10.1016/j.gr.2014.06.004.
Stern, R.J., 2002. Subduction zones. Rev. Geophys. 40 (4), 1–38. https://doi.org/10.1029/2001RG000108.
Stevens, C.H., Stone, P., Miller, J.S., 2005. A new reconstruction of the Paleozoic continental margin of southwestern North America: implications for the nature and timing of continental truncation and the possible role of the Mojave-Sonora megashear hypothesis. In: Anderson, T.H., Nourse, J.A., McKee, J.W., Steiner, M.B. (Eds.), The Mojave-Sonora Megashear Hypothesis: Development, Assessment, and Alternatives 393, 597–618. Geological Society of America Special Paper. https://doi.org/10.1130/0-8137-2393-0.597.
Stewart, J.H., Anderson, T.H., Haxel, G.B., Silver, L.T., Wrigth, J.E., 1986. Late Triassic paleogeography of the southern Cordillera: the problem of a source for voluminous volcanic detritus in the Chinle Formation of the Colorado Plateau region. Geology 14 (7), 567–570. https://doi.org/10.1130/0091-7613(1986)14<567:LTPOTS>2.0.CO;2.
Streckeisen, A., 1973. Plutonic rocks: classification and nomenclature recommended by the IUGS subcommission on the systematics of igneous rocks. Geotimes 18 (10), 26–30.
Streckeisen, A., 1976. To each plutonic rock its proper name. Earth Sci. Rev. 12 (1), 1–33. https://doi.org/10.1016/0012-8252(76)90052-0.
Streckeisen, A., Le Maître, R.W., 1979. A chemical approximation to the modal QAPF classification of the igneous rocks. Neues Jahrbuch fu¨r Mineralogie Abhandlungen 136, 169–206.
Sun, S.S., McDonough, W.F., 1989. Chemical and isotopic systematics of ocean basalts: implications for mantle composition and processes. In: Saunders, A.D., Norry, M.J. (Eds.), Magmatism in ocean basins 42, 313–345. Geological Society of London Special Publication. https://doi.org/10.1144/GSL.SP.1989.042.01.19.
Taylor, S.R., McLennan, S.M., 1985. The Continental Crust: its Composition and Evolution. Blackwell, Oxford, p. 312.
Tepper, J.H., Nelson, B.K., Bergantz, G.W., Irving, A.J., 1993. Petrology of the Chilliwack batholith, North Cascades, Washington: generation of calc-alkaline granitoids by melting of mafic lower crust with variable water fugacity. Contrib. Mineral. Petrol. 113, 333–351. https://doi.org/10.1007/BF00286926.
Thornton, C.P., Tuttle, O.F., 1960. Chemistry of igneous rocks. I differentiation index. Am. J. Sci. 258 (9), 664–684. https://doi.org/10.2475/ajs.258.9.664.
Torres, R., Ruiz, J., Patchett, P.J., Grajales, J.M., 1999. Permo-Triassic continental arc in eastern México: tectonic implications for reconstructions of southern North America. In: Bartolini, C., Wilson, J.L., Lawton, T.F. (Eds.), Mesozoic Sedimentary and Tectonic History of North-Central Mexico. Geological Society of America Special. Paper 340, 191–196. https://doi.org/10.1130/0-8137-2340-X.191.
Van der Lelij, R., Spikings, R., Ulianov, A., Chiaradia, M., Mora, A., 2016. Palaeozoic to early Jurassic history of the northwestern corner of Gondwana, and implications for the evolution of the Iapetus, Rheic and pacific oceans. Gondwana Res. 31, 271–294. https://doi.org/10.1016/j.gr.2015.01.011.
Viscarret, P., Wright, J., Urbani, F., 2009. New U-Pb zircon ages of el Baúl massif, cojedes state, Venezuela. Rev. Téc. Ing. Univ. Zulia. 32 (3), 210–221.
Vega-Granillo, R., Vidal-Solano, J.R., Solari, L.A., López-Martínez, M., Gómez-Juárez, O.S., Herrera-Urbina, S., 2013. Geochemical and geochronological constraints on the geologic evolution of the western Sonobari Complex, northwestern Mexico. Geol. Acta 11 (4), 443–463.
Velázquez-Santelíz, A.F., 2014. Efecto del basamento proterozoico sobre el magmatismo de arco cordillerano del SW de Norte América: Estudios en Sierra San Francisco, NW de Sonora [Tesis de Licenciatura]: Linares. Universidad Autónoma de Nuevo León, Facultad de Ciencias de la Tierra, p. 153.
Weber, B., Cameron, K.L., Osorio, M., Schaaf, P., 2005. A late permian tectonothermal event in grenville crust of the southern maya terrane: U–Pb zircon ages from the chiapas massif, southeastern Mexico. Int. Geol. Rev. 47, 509–529.
Wilson, M., 1989. Igneous Petrogenesis: A Global Tectonic Approach. Springer 2007, New York, p. 466.